



Discussion Paper

Estimating monthly Labour Force Figures during the COVID-19 pandemic in the Netherlands

Jan van den Brakel, Martijn Souren and Sabine Krieg

February 25, 2021

Abstract

Official monthly statistics about the Dutch labour force are based on the Dutch Labour Force Survey (LFS). The LFS is a continuously conducted survey that is designed as a rotating panel design. Data collection among selected households is based on a mixed-mode design that uses web interviewing, telephone interviewing and face-to-face interviewing. Monthly estimates about the labour force are obtained with a structural time series model. Due to the COVID-19 pandemic, face-to-face interviewing stopped. It was anticipated that this has a systematic effect on the outcomes of the LFS and that the lockdown at the same time effects the real monthly labour force figures. The lockdown indeed marked a sharp turning point in the evolution of the series of the monthly labour force figures and strongly increases the dynamics of these series. In this paper it is explained how Statistics Netherlands produces monthly labour force figures during the COVID-19 pandemic. It is shown how the sudden change in the mode effects, because face-to-face interviewing stopped, is separated from real period-to-period changes in the labour force figures. It is also explained how the time series model is adapted to the increased dynamics in the labour force figures.

1 Introduction

The purpose of the Dutch Labour Force Survey (LFS) is to publish reliable monthly, quarterly and annual figures about the Dutch labour force. The LFS is based on a rotating panel design. The responding households are interviewed five times at quarterly intervals, which implies that every month five waves are interviewed. In 2010, Statistics Netherlands implemented a model-based estimation procedure based on a multivariate structural time series model ([Durbin and Koopman, 2012](#)) to produce monthly figures about the labour force ([Pfeffermann, 1991](#); [van den Brakel and Krieg, 2015](#)). This model uses five series of GREG estimates observed in the waves of the rotating panel as input. This time series model is used as a form of small area estimation to produce sufficiently reliable monthly estimates, despite the relatively small monthly sample sizes. The model also accounts for systematic differences between the outcomes obtained in the subsequent waves. This is a well-known problem for rotating panel designs, known in the literature as rotation group bias (RGB), ([Bailar, 1975](#)). Finally the model accounts for systematic differences or discontinuities in the outcomes due to two major survey redesigns that took place in 2010 and 2012 ([van den Brakel and Roels, 2010](#)).

Data collection of the Dutch LFS is based on a sequential mixed-mode design that starts with Web Interviewing (WI). Non-respondents are followed up with computer assisted telephone interviewing (CATI) if a listed telephone number is available or with computer assisted personal interviewing (CAPI) otherwise.

Due to the COVID-19 pandemic, the Netherlands went in a lockdown on March 16, 2020. Due to this lockdown, CAPI stopped. Since this results in a sudden change in selection bias and measurement bias, this has a systematic effect on the outcomes of the LFS. At the same time, it can be expected that the lockdown effects the real monthly labour force figures. The Unemployed Labour Force time series show a steady decrease since 2014, while the evolution of the Employed Labour Force as well as the Total Labour Force show a steady increase during these last six years. The lockdown and its associated

policy measures indeed marked a sharp turning point in the evolution of these series and strongly increased the dynamics in the labour force series, which was, according to model diagnostics not sufficiently picked up by the time series model.

In this paper two problems related to the lockdown are addressed. The first problem is how to separate the sudden change in the mode effects because CAPI stopped from real period-to-period changes in the labour force figures. Extending the time series model with a level intervention variable is not a good solution, since the lockdown also resulted in a turning point at exactly the same time. In that case it can be expected that a major part of the real period-to-period change is incorrectly absorbed in the estimate for the regression coefficient of the level intervention that models the change in mode effects due to the loss of CAPI households. In this paper three different approaches to correct for the loss of CAPI responses are proposed and compared. The second problem is the abrupt turning point and sudden increase of the dynamics in the labour force figures due to the lockdown. Three different options are considered to accommodate for this in the time series model. It is discussed how the different approaches to account for both problems are evaluated during the first month of the lockdown in order to choose the most promising method for the publication of official monthly labour force figures. Consequences of these choices are discussed by comparing the different methods in an analysis that is conducted in real time until December 2020.

In Section 2, the survey design of the Dutch Labour Force Survey is described. The time series model used to produce official monthly figures about the labour force is described in Section 3. Several options that are considered to account for the sudden change in mode effects because face-to-face interviewing stopped, are described in Section 4 and in Section 5 a simulation and some first analysis results are presented to choose the best option. In Section 6 several options are described how the model can accommodate for the sudden increase in the dynamics of the population parameters. Results are presented in Section 7 and the report finalizes with a discussion in Section 8.

2 Dutch Labour Force Survey

The objective of the Dutch LFS is to provide reliable information about the Dutch labour force. Each month a stratified two-stage cluster sample of addresses is drawn. Strata are formed by geographical regions. Municipalities are considered as primary and addresses as secondary sampling units. All households residing at an address, up to a maximum of three, are included in the sample. Different subpopulations are oversampled to improve the accuracy of the official releases, for example, addresses where people live, who are formally registered at the employment office, and subpopulations with low response rates. Before 2000, the LFS was designed as a cross-sectional survey. Since October 1999, the LFS has been conducted as a rotating panel design. Until the redesign in 2010, data in the first wave were collected by means of CAPI. Respondents were re-interviewed four times at quarterly intervals by means of CATI. During these re-interviews, a condensed questionnaire was used to establish changes in the labour market position of the respondents.

In 2010, a major redesign for the LFS started. The main objective of this redesign was to reduce the administration costs of this survey. This is accomplished by changing the data collection in the first wave from CAPI to a mixed data collection mode using CAPI and CATI. Households with a listed telephone number are interviewed by telephone, the

remaining households are interviewed face-to-face. To make CATI data collection in the first wave feasible, the questionnaire for the first wave needed to be abridged since it is Statistics Netherlands policy that telephone interviews should not take longer than 15 to 20 minutes. Therefore, parts of the questionnaire were transferred from the first to the second or third interview round.

In 2012, a second major redesign of the LFS took place. Data collection in the first wave changed to a sequential mixed-mode design that starts with WI. After three reminders the non-responding households are contacted by telephone if they have a listed telephone number. The remaining households are interviewed face-to-face. It was again necessary to change the questionnaire in all the five waves. Data collection in the re-interviews remained CATI after both redesigns.

The aforementioned redesigns have systematic effects on the sample estimates of the survey. These so-called discontinuities were quantified by collecting data under the old and new design alongside each other for some period of time. This is referred to as parallel data collection or parallel run. In case of both redesigns, a parallel run was conducted for the first wave for a period of six months where the sample sizes assigned to the old and new design were both equal to the regular sample size. Based on these parallel runs, direct estimates for the discontinuities are obtained and used in the time series model described in Section 3.

The monthly gross sample size for the first wave averaged about 8,000 households commencing the moment that the LFS changed to a rotating panel design and gradually fell to about 6,500 households in 2012. The response rate was about 55% in the first wave and in the subsequent waves about 90% with respect to the responding households from the preceding wave. After the second redesign in 2012, the monthly sample size in the first wave increased to about 8500 households. Response rates in the first wave vary between 50% and 55%. In the second wave a response of about 70% of the households that responded to the first wave is obtained. In the third, fourth and fifth waves about 90% response is obtained among the households that responded to the preceding wave.

Key parameters of the LFS are the Employed, Unemployed and Total Labour Force, which are defined as population totals. Another important parameter is the Unemployment Rate, which is defined as the ratio of the Unemployed Labour Force to the Total Labour Force. These figures are estimated on a monthly frequency at the national level and a breakdown in six domains that is based on the cross classification of gender and age in three age classes.

Due to the COVID-19 pandemic, the Netherlands went in a lockdown at 16th March 2020. CAPI interviewing stopped at that moment. In an attempt to obtain as much as possible responses from the households that are originally assigned to CAPI, households are sent a letter with the request to contact the interviewer assigned to them, so that they can call back to conduct the interview by telephone. In September 2020, CAPI was started up again. In the third week of December a second lockdown started and CAPI interviewing stopped again. The effects of this second lockdown are further described in this paper, since the analysis is based on the data observed until December.

3 Time series model for monthly labour force figures

Monthly figures about the labour force are based on a structural time series model. According to the rotation scheme of the panel design, households are interviewed five times at quarterly intervals. This implies that each month data are collected in five independent samples. For each sample direct estimates for the monthly Employed Labour Force, Unemployed Labour Force, and Total Labour Force are obtained with the general regression (GREG) estimator ([Särndal et al., 1992](#)). Inclusion probabilities reflect the sampling design and differences in response rates between geographic regions. The weighting scheme of the GREG estimator is based on a combination of different socio-demographic categorical variables. Let $\hat{y}_t^{[j]}$ denote the GREG estimate for the unknown population parameter, say θ_t , based on the j -th wave observed in month t , $j = 1, \dots, 5$. Since responding households are interviewed at quarterly intervals, it follows that the j -th wave interviewed in month t was sampled for the first time in month $t - 3j + 3$. The GREG estimates of each month can be expressed as a vector $\hat{y}_t = (\hat{y}_t^{[1]}, \dots, \hat{y}_t^{[5]})'$. This five dimensional time series with GREG estimates is the input for a multivariate structural time series model, initially proposed by [Pfeffermann \(1991\)](#) for this kind of time series to model the population parameter of interest, and to account for the RGB and the autocorrelation in the sampling errors. This approach is extended with intervention components to model the discontinuities of the survey redesigns in 2010 and 2012. The model outlined in this Section is described in more detail in [van den Brakel and Krieg \(2015\)](#). The following time series model for the five series of GREG estimates is applied to the monthly target variables of the Dutch LFS:

$$\hat{y}_t = j_{[5]}\theta_t + \lambda_t + \Delta_t^{[1]}\beta_t^{[1]} + \Delta_t^{[2]}\beta_t^{[2]} + e_t, \quad (1)$$

with $j_{[5]}$ a five dimensional column vector with each element equal to one, $\lambda_t = (\lambda_t^{[1]}, \lambda_t^{[2]}, \lambda_t^{[3]}, \lambda_t^{[4]}, \lambda_t^{[5]})'$ a vector with time dependent components that account for the RGB, $\Delta_t^{[i]} = \text{Diag}(\delta_t^{[i,1]}, \delta_t^{[i,2]}, \delta_t^{[i,3]}, \delta_t^{[i,4]}, \delta_t^{[i,5]})$ a diagonal matrix with dummy variables that change from zero to one at the moment that the survey changes from the old to the new design during redesign $i = 1$ in 2010 and $i = 2$ in 2012, $\beta_t^{[i]} = (\beta_t^{[i,1]}, \beta_t^{[i,2]}, \beta_t^{[i,3]}, \beta_t^{[i,4]}, \beta_t^{[i,5]})'$ a five dimensional vector with regression coefficients, $i = 1, 2$, and $e_t = (e_t^{[1]}, e_t^{[2]}, e_t^{[3]}, e_t^{[4]}, e_t^{[5]})'$ the corresponding survey errors for each wave estimate. The information obtained during the parallel run in the first wave is used as a priori information in the model and the regression $\beta_t^{[i,1]}$ is made time varying during the period of the parallel run, $i = 1, 2$. See [van den Brakel and Krieg \(2015\)](#) for details.

The population parameter θ_t in (1) can be decomposed in a trend component, a seasonal component, and an irregular component, i.e.

$$\theta_t = L_t + S_t + \epsilon_t. \quad (2)$$

In (2), L_t is the so-called smooth trend model, which is defined as

$$\begin{aligned} L_t &= L_{t-1} + R_{t-1} \\ R_t &= R_{t-1} + \eta_t \quad \eta_t \simeq N(0, \sigma_\eta^2) \end{aligned} \quad (3)$$

Furthermore, S_t in (2) denotes a trigonometric stochastic seasonal component, which is defined as

$$\begin{aligned} S_t &= \sum_{j=1}^{J/2} \gamma_{j,t}, \text{ with} \\ \gamma_{j,t} &= \gamma_{j,t-1} \cos(2\pi j/J) + \gamma_{j,t-1}^* \sin(2\pi j/J) + \omega_{j,t} \\ \gamma_{j,t}^* &= \gamma_{j,t-1}^* \cos(2\pi j/J) - \gamma_{j,t-1} \sin(2\pi j/J) + \omega_{j,t}^* \\ \omega_{j,t} &\simeq N(0, \sigma_\omega^2) \quad \omega_{j,t}^* \simeq N(0, \sigma_\omega^2), \quad j = 1, \dots, J/2. \end{aligned} \quad (4)$$

For monthly time series, $J = 12$. Finally, ϵ_t in (2) denotes the irregular component, which contains the unexplained variation of the population parameter and is modelled as a white noise process, i.e. $\epsilon_t \simeq N(0, \sigma_\epsilon^2)$.

The systematic differences between the subsequent waves, i.e. the RGB, are modelled in (1) with λ_t . The absolute bias in the monthly labour force figures cannot be estimated from the sample data only. Therefore, additional restrictions for the elements of λ_t are required to identify the model. Here it is assumed that an unbiased estimate for θ_t is obtained with the first wave, i.e. $\hat{y}_t^{[1]}$, see [van den Brakel and Krieg \(2009\)](#) for a motivation. This implies that the first component of λ_t equals zero. The other elements of λ_t measure the time dependent differences with respect to the first wave and are modelled as random walks. As a result,

$$\lambda_t^{[1]} = 0, \quad \lambda_t^{[j]} = \lambda_{t-1}^{[j]} + \eta_{\lambda,t}^{[j]}, \quad j = 2, 3, 4, 5, \quad \eta_{\lambda,t}^{[j]} \simeq N(0, \sigma_\lambda^2). \quad (5)$$

Note that the disturbance terms of the random walks for the RGB in waves 2, 3, 4 and 5 share the same variance component σ_λ^2 .

The discontinuities induced by the redesigns in 2010 and 2012 are modelled with the third and fourth term in (1). The diagonal matrix $\Delta_t^{[i]}$ contains five intervention variables:

$$\delta_t^{[i,j]} = \begin{cases} 0 & \text{if } t < T_{R_i}^{[j]} \\ 1 & \text{if } t \geq T_{R_i}^{[j]} \end{cases}, \quad (6)$$

where $T_{R_i}^{[j]}$ denotes the moment that wave j changes from the old to the new survey design in redesign $i = 1$ in 2010 or $i = 2$ in 2012. Under the assumption that (2) correctly models the evolution of the population variable, the regression coefficients in $\beta_t^{[i]}$ can be interpreted as the systematic effects of the redesign on the level of the series observed in the five waves. The intervention approach with state-space models was originally proposed by [Harvey and Durbin \(1986\)](#) to estimate the effect of seat belt legislation on British road casualties. With level intervention (6), it is assumed that the redesign only has a systematic effect on the level of the series. Alternative interventions, e.g. for the slope or the seasonal components are also possible, see [Durbin and Koopman \(2012\)](#), Ch. 3. A redesign might not only affect the point estimates, but also the variance of the GREG estimates. This issue is discussed under the time series model for the survey errors.

The last component in (1) is a time series model for the survey errors. The estimates for the design variances of the sampling errors are available from the micro data and are incorporated in the time series model using the survey error model $e_t^{[j]} = k_t^{[j]} \hat{e}_t^{[j]}$ where $k_t^{[j]} = \sqrt{\widehat{var}(\hat{y}_t^{[j]})}$. Here $\widehat{var}(\hat{y}_t^{[j]})$ denotes the estimated variance of the GREG

estimates $\hat{y}_t^{[j]}$. Choosing the survey errors proportional to the standard error of the GREG estimators allows for heterogeneous variance in the survey errors, that arise e.g. due to the gradually changing sample sizes over time.

The sample of the first wave has no sample overlap with waves observed in the past. Consequently, the survey errors of the first wave, $e_t^{[1]}$, are not correlated with survey errors in the past. It is, therefore, assumed that $\tilde{e}_t^{[1]}$ is white noise, i.e. $\tilde{e}_t^{[1]} \simeq N(0, \sigma_{e_1}^2)$. As a result, the variance of the survey error equals $\text{var}(e_t^{[1]}) = (k_t^{[1]})^2 \sigma_{e_1}^2$, which is approximately equal to the direct estimate of the variance of the GREG estimate for the first wave if the maximum likelihood (ML) estimate for $\sigma_{e_1}^2$ is close to one.

The survey errors of the second, third, fourth and fifth wave are correlated with survey errors of preceding periods. The autocorrelations between the survey errors of the subsequent waves are estimated from the survey data, using the approach proposed by [Pfeffermann et al. \(1998\)](#). In this application, it appears that the autocorrelation structure for the second, third, fourth and fifth wave can be modelled conveniently with an AR(1) model, [van den Brakel and Krieg \(2015\)](#). Therefore, it is assumed that $\tilde{e}_t^{[j]} = \rho \tilde{e}_{t-3}^{[j-1]} + v_t^{[j]}$, with ρ the first order autocorrelation coefficient, and $v_t^{[j]} \simeq N(0, \sigma_{e_j}^2)$ for $j = 2, 3, 4, 5$. Since $\tilde{e}_t^{[j]}$ is an AR(1) process, $\text{var}(e_t^{[j]}) = (k_t^{[j]})^2 \sigma_{e_j}^2 / (1 - \rho^2)$. As a result, $\text{var}(e_t^{[j]})$ is approximately equal to $\widehat{\text{var}}(\hat{y}_t^{[j]})$ provided that the ML estimates for $\sigma_{e_j}^2$ are close to $(1 - \rho^2)$.

The survey redesign in 2010 and 2012 might affect the variance of the GREG estimates. Systematic differences in these variances are automatically taken into account by this model. An alternative would be to allow for different values for $\sigma_{e_j}^2$ for the periods with different survey design, which can be interpreted as interventions on the variance hyperparameters of the survey errors.

The general way to proceed is to express the model in the so-called state space representation and apply the Kalman filter to obtain optimal estimates for the state variables, see e.g. [Durbin and Koopman \(2012\)](#). It is assumed that the disturbances are normally distributed. Under this assumption, the Kalman filter gives optimal estimates for the state vector and the signals. Estimates for state variables for period t based on the information available up to and including period t are referred to as the filtered estimates. The filtered estimates of past state vectors can be updated if new data become available. This procedure is referred to as smoothing and results in smoothed estimates that are based on the completely observed time series. In this application, interest is mainly focused on the filtered estimates, since they are based on the complete set of information that would be available in the regular production process to produce a model-based estimate for month t .

The analysis is conducted with software developed in OxMetrics in combination with the subroutines of SsfPack 3.0, see [Doornik \(2009\)](#) and [Koopman et al. \(2008\)](#). All state variables are non-stationary with the exception of the survey errors and the population white noise. The non-stationary variables are initialised with a diffuse prior, i.e. the expectation of the initial states are equal to zero and the initial covariance matrix of the states is diagonal with large diagonal elements. The survey errors are stationary and therefore initialised with a proper prior. The initial values for the survey errors are equal to zero and the covariance matrix is available from the aforementioned model for the survey errors. In Ssfpack 3.0, an exact diffuse log-likelihood function is obtained with the procedure proposed by [Koopman \(1997\)](#).

The following publications for the monthly labour force are derived from this model. For

the Unemployed Labour Force, Employed Labour Force and the Total Labour Force, a trend-cycle (L_t) and a trend-cycle plus seasonal ($L_t + S_t$) is published. In this paper the trend-cycle is briefly referred to as the trend and the trend-cycle plus seasonal is further referred to as the signal. Trends and signals are estimated for these three target variables at the national level and for a breakdown in six domains that is based on the cross-classification of gender and three age classes. A Lagrange function is applied to ensure that the sum over the domain totals equals the national totals, and to ensure that the sum of the Employed and Unemployed Labour Force is exactly equal to the Total Labour Force, both at national and domain level. See [van den Brakel and Krieg \(2015\)](#) for details.

4 Estimating change in mode effects

Suddenly stopping CAPI data collection because of the lockdown has a similar effect as the redesigns of the survey process in 2010 and 2012. It results in a sudden change of measurement bias and selection bias in the responses of the LFS and therefore has a systematic effect on the sample estimates. In a well-planned transition process, this is anticipated by quantifying these discontinuities to avoid confounding real developments with systematic effects induced by the redesign ([van den Brakel et al., 2020](#)). A safe approach to quantify discontinuities is to conduct a parallel run (see Section 2). Another approach is to quantify discontinuities by fitting a structural time series model, containing intervention variables to account for discontinuities, as explained in Section 3 for the two redesigns in 2010 and 2012. This approach is cost effective, since no additional data collection is required, but relies on the strong assumption that during the change-over the time series model correctly describes the evolution of the population parameter. All deviations from this evolution are interpreted by the model as a discontinuity due to the redesign and are absorbed in the regression coefficient of the level intervention. If the change-over exactly coincides with a turning point, it can be expected that a part of the real period-to-period change is incorrectly absorbed in the regression coefficient of the level intervention. This will result in a biased estimate for the discontinuity and the model predictions for the population parameter.

As explained in Section 3, the population parameter estimates in the time series model are benchmarked to the level of the series observed in the first wave, since it is assumed that the RGB in the first wave equals zero. It is therefore crucial that the first wave is measured as accurately as possible, including possible discontinuities due to a redesign. Therefore, it was in 2010 and 2012 decided to allocate the available budget for a parallel run for the first wave exclusively. In both transitions, the first wave was conducted in parallel for a period of six months at the size of the regular survey. This resulted in sufficiently precise estimates for the discontinuities in the first wave, which are used as a priori information for $\beta_t^{[1,1]}$ and $\beta_t^{[2,1]}$ in model (1). The regression coefficients of the intervention variables for the follow up waves are estimated with the Kalman filter, see [van den Brakel and Krieg \(2015\)](#) for details.

In an attempt to reduce the loss of CAPI households, these households were send additional letters to motivate them to contact Statistics Netherlands by telephone to complete the questionnaire via CATI. At the same time different strategies to account for the change in mode effects in the estimation approach were developed. A standard intervention approach is not appropriate to estimate the discontinuity due to the loss of

CAPi households directly after the lockdown because the lockdown also has a strong effect on the real period-to-period change of the labour force figures. As will be shown later, the lockdown indeed marks a sharp turning point the series of the labour force figures. Three approaches are identified to separate a sudden change in mode effects from the real period-to-period change of the target variables.

The lockdown started at March 16. The major part of the CAPI households were approached before this date and a response of 22% was obtained. On average the response among the CAPI households is 40%. It was decided to treat March as a normal month and account for the loss of CAPI from April 2020 on. This decision was supported since the period-to-period change of the Unemployed Labour Force from February to March was in line with the claimant count figures if March was treated as a normal month with complete response of all three modes. Also DEcember was treated as a normal month.

Option 1: using CATI en WI respondents in wave 1 only

Under this option only the original WI and CATI respondents in wave 1 are used for the period from April up until August 2020. All households originally assigned to CAPI are ignored, including the CAPI households that agreed to participate via CATI. Model 1 is extended with an additional component that models the discontinuity due to the loss of CAPI households in the first wave, i.e.

$$\hat{y}_t = j_{[5]} \theta_t + \lambda_t + \Delta_t^{[1]} \beta_t^{[1]} + \Delta_t^{[2]} \beta_t^{[2]} + \Delta_t^{[3]} \beta_t^{[3]} + e_t, \quad (7)$$

The diagonal matrix $\Delta_t^{[3]}$ contains five intervention variables:

$$\delta_t^{[3,j]} = \begin{cases} 0 & \text{if } t \notin [T_{LD} + (j-1) * 3, \dots, T_{LD} + (j-1) * 3 + \tau] \\ 1 & \text{if } t \in [T_{LD} + (j-1) * 3, \dots, T_{LD} + (j-1) * 3 + \tau] \end{cases}, j = 1, \dots, 5, \quad (8)$$

where T_{LD} denotes April 2020, the month that CAPI response is completely missing for the first time and τ the number of months without CAPI respondents in the first wave. In this application $\tau=5$, since CAPI was started again in September. Note that discontinuities are also expected in the follow up waves, since the loss of CAPI households also has a selection effect in the follow up waves. Furthermore, the vector $\beta^{[3]} = (\beta^{[3,1]}, \beta^{[3,2]}, \beta^{[3,3]}, \beta^{[3,4]}, \beta^{[3,5]})'$ contains the selection effects or discontinuities due to loss of the CAPI households in the first wave.

As emphasized before, estimating the discontinuities $\beta^{[3]}$ due to the loss of CAPI by applying the Kalman filter to a state-space version of model (7), results in biased estimates since the start of the lockdown also marks a sharp turning point in the real evolution of the target variable. However, the discontinuities due to the loss of CAPI households can be estimated in a reliable way using a separate time series model. Starting with the first wave, two time series of direct estimates are constructed, one with and one without CAPI respondents. This can also be done for the follow up waves; one time series based on the full response and one time series where the CAPI respondents from the first wave are left out. This series is available from 2012 which is the moment of the change-over to the sequential mixed-mode design that is based on WI, CATI and CAPI. In this way, for each wave, a parallel run of about 8 years is created. It is, however, anticipated that the composition of the modes gradually changes over this long period, resulting in time varying differences between the two series of GREG estimates. Both series are combined in a three dimensional time series model, which

also contains a series of claimant counts as an auxiliary series:

$$\begin{pmatrix} \hat{y}_t^{[j]} \\ \hat{y}_t^{[j]*} \\ x_t \end{pmatrix} = \begin{pmatrix} L_t^y \\ L_t^y \\ L_t^x \end{pmatrix} + \begin{pmatrix} 0 \\ \kappa_t^{[j]} \\ 0 \end{pmatrix} + \begin{pmatrix} S_t^y \\ S_t^y \\ S_t^x \end{pmatrix} + \begin{pmatrix} e_t^y \\ e_t^{y*} \\ e_t^x \end{pmatrix}, t = T_{R_2}^j \dots T_{LD} + 3 * (j - 1) - 1. \quad (9)$$

This model is applied to the series of each wave separately and it is understood that L_t^y , S_t^y , e_t^y , and e_t^{y*} are therefore wave dependent but that the superscripts that indicate the j -th wave are suppressed for notational convenience. In (9) $\hat{y}_t^{[j]}$ denotes the direct estimate in month t based on the complete response, $\hat{y}_t^{[j]*}$ the direct estimate in month t based on the WI and CATI respondents in the first wave only, and x_t the claimant counts for month t . The two LFS series share the same smooth trend model L_t^y , as defined in (3), and the same trigonometric seasonal component S_t^y , as defined in (4). The systematic difference between $\hat{y}_t^{[j]}$ and $\hat{y}_t^{[j]*}$ is modelled with a random walk, $\kappa_t^{[j]}$, i.e.

$$\kappa_t^{[j]} = \kappa_{t-1}^{[j]} + \eta_{\kappa,t}, \quad \eta_{\kappa,t} \simeq N(0, \sigma_\kappa^2), \quad (10)$$

and has in fact the same interpretation as the RGB in (5). In the case that σ_κ^2 turns out to be small, such that $\kappa_t^{[j]}$ follows a relative smooth pattern, the final value for $\kappa_t^{[j]}$ can be used as an estimate for the discontinuities $\beta^{[3,j]}$ in (7). In case of an erratic pattern, a smooth trend model for $\kappa_t^{[j]}$ could be considered as an alternative. The claimant counts series has its own smooth trend L_t^x , which is similarly defined as (3), and its own trigonometric seasonal component S_t^x , which is similarly defined as (4). The claimant count series serves as an auxiliary series to obtain more precise estimates for $\kappa_t^{[j]}$. This is achieved by modeling the correlation, say ρ , between the slope disturbance terms of L_t^y and L_t^x . If η_t^y and η_t^x denote the slope disturbance terms for the LFS trend and the claimant counts trend in (3) respectively, then it is assumed that

$$\begin{pmatrix} \eta_t^y \\ \eta_t^x \end{pmatrix} \simeq N \left(\begin{pmatrix} 0 \\ 0 \end{pmatrix}, \begin{pmatrix} \sigma_{\eta_y}^2 & \rho \sigma_{\eta_y} \sigma_{\eta_x} \\ \rho \sigma_{\eta_y} \sigma_{\eta_x} & \sigma_{\eta_x}^2 \end{pmatrix} \right).$$

Finally e_t^y , e_t^{y*} and e_t^x are the measurement errors of respective series $\hat{y}_t^{[j]}$, $\hat{y}_t^{[j]*}$, and x_t . For e_t^x it is assumed that $e_t^x \simeq N(0, \sigma_{e_x}^2)$ and are not correlated with e_t^y and e_t^{y*} . The measurement errors of the LFS series are dominated by the sampling error and are also correlated since the WI and CATI respondents in $\hat{y}_t^{[j]}$ and $\hat{y}_t^{[j]*}$ are the same persons. For e_t^y and e_t^{y*} it is assumed that $e_t^y \simeq N(0, \widehat{var}(\hat{y}_t^{[j]})\sigma_e^2)$ and $e_t^{y*} \simeq N(0, \widehat{var}(\hat{y}_t^{[j]*})\sigma_{e^*}^2)$. Similarly as in the production model, $\widehat{var}(\hat{y}_t^{[j]})$ and $\widehat{var}(\hat{y}_t^{[j]*})$ are estimated using the sample data and are used as a priori information in the time series model. The covariance between e_t^y and e_t^{y*} is approximated as

$$\widehat{cov}(\hat{y}_t^{[j]}, \hat{y}_t^{[j]*}) = \tilde{\rho} \frac{n_t^{o.l.}}{\sqrt{n_t n_t^*}} \sqrt{\widehat{var}(\hat{y}_t^{[j]})} \sqrt{\widehat{var}(\hat{y}_t^{[j]*})}, \quad (11)$$

where $\tilde{\rho}$ is the correlation based on the sample overlap of $\hat{y}_t^{[j]}$ and $\hat{y}_t^{[j]*}$, n_t the sample size used to estimate $\hat{y}_t^{[j]}$, i.e. the complete sample in month t including the CAPI respondents, n_t^* the sample size used to estimate $\hat{y}_t^{[j]*}$, i.e. the sample in month t with the WI and CATI respondents only, and $n_t^{o.l.}$ the number of sample units that appear both in the sample used to estimate $\hat{y}_t^{[j]}$ and $\hat{y}_t^{[j]*}$. Note that the sample overlap are the

WI and CATI respondents in the sample of month t . As a result, $\tilde{\rho} = 1$ and $n_t^{o.l.} = n_t^*$. Therefore (11) simplifies to

$$\widehat{cov}(\hat{y}_t^{[j]}, \hat{y}_t^{[j]*}) = \frac{\sqrt{n_t^*}}{\sqrt{n_t}} \sqrt{\widehat{var}(\hat{y}_t^{[j]})} \sqrt{\widehat{var}(\hat{y}_t^{[j]*})}. \quad (12)$$

The series used in (9) start in the month in 2012 that wave j changed to the sequential mixed mode design that is based on WI, CATI and CAPI, i.e. $t = T_{R_2}^{[j]}$, until the period that the complete response has been observed, i.e. $t = (T_{LD} + 3 * (j - 1) - 1)$. The estimate for $\kappa_t^{[j]}$ obtained for the last period with complete response with model (9) is used as a priori available information for $\beta^{[3,j]}$ in model (7) via an exact initialization of the Kalman filter.

The advantage of Option 1 is that there is a long series of 8 years available that can be used to estimate the discontinuity due to the loss of the CAPI respons in the first wave. The disadvantage of this option is that the responses obtained from the CAPI respondents that agreed to complete a questionnaire by CATI, are not used.

Option 2: using CATI en WI respondents and CAPI households in wave 1 that respond by CATI

Under this option all responses obtained in wave 1 are used, i.e. the WI and CATI respondents and the respondents that originally were assigned to the CAPI mode, but agreed to participate via CATI. In this case, compared to Option 1, a different discontinuity is introduced. The discontinuity in wave 1 is the net result of changing measurement bias, since a part of the CAPI households participate via CATI, and changing selection bias, since not all CAPI households will contact Statistics Netherlands to participate via CATI. The discontinuities in the follow up waves are mainly the result of increased selection bias due to the loss of response of the CAPI households in the first wave.

Under this option, production model (1) is extended with a component that accounts for the aforementioned discontinuities in an equivalent way as Model (7) under Option 1. The discontinuities are estimated in a separate model, which is an extension of Model (9) and is defined as:

$$\begin{pmatrix} \hat{y}_t^{[j]} \\ \hat{y}_t^{[j]*} \\ x_t \end{pmatrix} = \begin{pmatrix} L_t^y \\ L_t^y \\ L_t^x \end{pmatrix} + \begin{pmatrix} 0 \\ \kappa_t^{[j]} \\ 0 \end{pmatrix} + \begin{pmatrix} \beta^{[3,j]} \delta_t^{[3,j]} \\ 0 \\ 0 \end{pmatrix} + \begin{pmatrix} S_t^y \\ S_t^y \\ S_t^x \end{pmatrix} + \begin{pmatrix} e_t^y \\ e_t^{y*} \\ e_t^x \end{pmatrix}, t = T_{R_2}^{[j]} \dots T, \quad (13)$$

with $\delta_t^{[3,j]}$ defined in (8). The difference with Option 1 is that this model runs until the last available observation, instead of the moment that in wave j the CAPI households from the first wave are missing. Furthermore, model (9) is extended with a level shift $\beta^{[3,j]} \delta_t^{[3,j]}$, that estimates the break in wave j since from period $T_{LD} + 3 * (j - 1)$, the CAPI households are missing or participate via CATI in the series of y_t^j . The estimate for $\beta^{[3,j]}$ obtained with model (13) is used as a priori available information for $\beta^{[3,j]}$ in Model (7) via an exact initialization of the Kalman filter. Similar to Model (9), Model (13) is applied to the series of each wave separately. Therefore L_t^y , S_t^y , e_t^y , and e_t^{y*} are in fact wave dependent but the superscripts that indicate the j -th wave are suppressed for notational convenience.

The advantage of this approach is that the CAPI households that decided to participate via CATI are also used in the estimation of the monthly figures. The major drawback of

this approach is that the estimates for $\beta^{[3,j]}$ are highly unstable. In the first month of the lockdown there is only one observation for $\beta^{[3,1]}$ in the first wave. These estimates will be subject to large revisions if additional observations become available in the subsequent months. A possible solution is to use Option 1 for one quarter and change to Option 2 in the fourth month of the lockdown.

Option 3: the follow up waves are leading

As emphasized in Section 3, the results obtained in the first wave are considered to be more reliable compared to the results in the follow-up waves. Therefore, the outcomes of the follow-up waves are benchmarked to the first wave in (1) by assuming that the RGB in the first wave is zero. It can be argued that due to the sudden loss of CAPI in the first wave, the outcomes of the follow-up waves are more reliable than the first wave. An alternative approach, therefore, is to allow RGB for the first wave and make one of the follow-up waves leading. The RGB for the follow-up waves are not significantly different during the years before the lockdown. It is therefore a natural choice to set the RGB for all follow-up waves equal to zero. This implies that the level of the population parameter θ_t is benchmarked to the average of the series of the follow-up waves. In this case, the RGB in Model (7) is defined as $\lambda_t = (\lambda_t^{[1]}, 0, 0, 0, 0)'$. Estimates for the discontinuities due to the lockdown, i.e. $\beta_t^{[3]}$ in (7) can be obtained using either the method proposed under Option 1 or Option 2.

To maintain uninterrupted series, the population parameter estimates must refer to the level of the first wave. This implies that under this option the published trend estimates for target variables are obtained by $L_t + \lambda_t^{[1]}$ and signal estimates by $L_t + S_t + \lambda_t^{[1]}$.

Assumptions

All three options require strong assumptions to disentangle change in mode effects from real period-to-period change. More precisely, it is assumed that the difference between the outcomes of the first wave with and without CAPI is not affected by the lockdown. This assumption is required to project the estimated difference in the first wave with and without CAPI to the period during the lockdown. This also implies that it is assumed that the WI and CATI response before and after the start of the lockdown are comparable. Similar assumptions are made for the follow-up waves. Finally it is assumed that the autocorrelation in the survey errors and the seasonal component are not affected by the lockdown. More observations after the start of the lockdown are required to establish effects on the autocorrelation and the seasonal component. Under option 3 it is also assumed that the RGB component for the first wave is not affected by the lockdown.

5 Choosing the optimal approach

Simulations

In preparation of the first publication under the lockdown, i.e. April 2020, a simulation study is conducted to choose the most appropriate option once the data over April become available in the first week of May. In this simulation filtered trends, estimated in real time are analyzed. The simulation is set up as follows. The starting point are the series observed with the Dutch LFS up until March 2020. In this simulation it is assumed that the corona pandemic started in December 2019. A turning point is created by

assuming a monthly increase of 30,000 for the Unemployed Labour Force over the last four months. This means that in December 2019, 30,000 unemployed are added to the five input series. Similarly 60,000, 90,000 and 120,000 unemployed are added in January, February and March 2020 respectively. This comes down to a simulated monthly increase of 10%, since the level of the Unemployed Labour Force in December was about 300,000 people. In a similar way a monthly decrease of 30,000 people is simulated for the series of the Employed Labour Force over the last four months. This implies that the input series for the Employed Labour Force are decreased with 30,000 in December 2019. This value gradually increased to 120,000 in March 2020. This comes down to a monthly decrease of 0,3%. For the Total Labour Force a monthly decrease of 100,000 people is simulated. Thus for this variable the input series in December 2019 are decreased with 100,000 people. This value gradually increased to 400,000 in March 2020. This comes down to a monthly decrease of 1%. It is understood that the chosen values for the corona impact are not consistent, since the restriction that the sum of the Unemployed and Employed Labour Force is equal to the Total Labour Force is not obeyed. For the purpose of this simulation, this doesn't matter, since the main goal is to test the options under different amounts of impact of the corona crisis on the LFS series. In the next step, trends are estimated using the series where the above mentioned turning points are added applied to Model (1). These trends are used as the benchmark in the evaluation of the three aforementioned options, since they reflect the estimated trends in case of a turning point if nothing changes in the data collection. These trends are further referred to as the benchmark trend. Subsequently an in real time analysis is conducted with all three options.

For Option 1, trend estimates are made in real time using GREG estimates based on WI and CATI only for December 2019 up until March 2020, using Model (7). The break due to the loss of CAPI equals the value for $\kappa_t^{[1]}$ at November 2019, obtained with Model (9). The in real time estimated trends under Option 1 are compared with the benchmark trend in Table 5.1.

For Option 2, turning points are created as described above. Subsequently discontinuities with three different values are added to the first wave to simulate the effect that a small fraction of CAPI households participate through CATI and the nonresponse among CAPI households increases. For the Unemployed Labour Force, a discontinuity of 50,000, 0, and -50,000 is simulated. For the Employed Labour Force and Total Labour Force values of 75,000, 0, and -75,000 are simulated. Subsequently, trend estimates are made in real time using GREG estimates based on WI, CATI, and CAPI plus the simulated discontinuities for December 2019 up until March 2020, using Model (7). The break due to the loss of CAPI equals the value for $\beta^{[3,1]}$, estimated in real time with Model (13). The in real time estimated trends under Option 2 are compared with the benchmark trend in Table 5.2. Results are presented for a simulation with a discontinuity in the first wave of 50,000 for the Unemployed Labour Force and 75,000 for the Employed Labour Force and the Total Labour Force. Results for values equal to zero and -50,000 or -75,000 are very similar and therefore omitted.

The third option is evaluated in combination with Option 2, i.e. during the lockdown the CAPI households that agreed to participate via CATI are used in the GREG estimator for the first wave. The values for the discontinuities used in the simulation are similar to the values used under Option 2. Subsequently, trend estimates are made in real time using GREG estimates based on WI, CATI, and CAPI plus the simulated discontinuities for December 2019 up until March 2020, using Model (7) with $\lambda_t = (\lambda_t^{[1]}, 0, 0, 0, 0)'$. The

trend is now defined as $L_t + \lambda_t^{[1]}$ as explained under Option 3. The break due to the loss of CAPI equals the value for $\beta^{[3,1]}$, estimated in real time with Model (13). The in real time estimated trends under Option 3 are compared with the benchmark trend in Table 5.3. As in the case of the simulation with Option 2, results are presented for discontinuities with values 50,000 for the Unemployed and 75,000 for the Employed and Total Labour Force. The other values for the discontinuities gives comparable results and are omitted.

	Difference trend with benchmark trend			
	December 2019	January 2020	February 2020	March 2020
Last observed month	Results Unemployed Labour Force			
December 2019	-2990			
January 2020	-3195	873		
February 2020	-3772	154	-3690	
March 2020	-3864	96	-4010	-3649
	Results Employed Labour Force			
December 2019	-4802			
January 2020	-4620	-17912		
February 2020	-4296	-17210	-20889	
March 2020	-3880	-16888	-19776	-15856
	Results Total Labour Force			
December 2019	-28843			
January 2020	-27788	-71676		
February 2020	-17695	-43930	-70038	
March 2020	-8984	-19077	-25628	-17735

Table 5.1 Simulation results Option 1: real time estimates for the differences between the trend and the benchmark trends for Unemployed Labour Force, Employed Labour Force and Total Labour Force at the national level. The last four columns contain differences for respectively December, January, February, and March, based on the time series observed until the month specified in the first column.

	Difference trend with benchmark trend			
	December 2019	January 2020	February 2020	March 2020
Last observed month	Results Unemployed Labour Force			
December 2019	-3326			
January 2020	-203	-557		
February 2020	-2093	-3525	-4945	
March 2020	-2056	-3463	-5017	-5054
	Results Employed Labour Force			
December 2019	-3300			
January 2020	-4930	-11194		
February 2020	-4985	-11460	-17032	
March 2020	-3471	-8338	-11792	-12148
	Results Total Labour Force			
December 2019	-28930			
January 2020	-28210	-73115		
February 2020	-19670	-49102	-78026	
March 2020	-8860	-19363	-26423	-25480

Table 5.2 Simulation results Option 2: real time estimates for the differences between the trend and the benchmark trends for Unemployed Labour Force, Employed Labour Force and Total Labour Force at the national level. The last four columns contain differences for respectively December, January, February, and March, based on the time series observed until the month specified in the first column.

	Difference trend with benchmark trend			
	December 2019	January 2020	February 2020	March 2020
Last observed month	Results Unemployed Labour Force			
December 2019	-10800			
January 2020	-6940	-11530		
February 2020	-9380	-15450	-15700	
March 2020	-9390	-15525	-15850	-17570
	Results Employed Labour Force			
December 2019	-13560			
January 2020	-15670	-22985		
February 2020	-15690	-23216	-25943	
March 2020	-14040	-19576	-19950	-23570
	Results Total Labour Force			
December 2019	-46525			
January 2020	-46748	-99064		
February 2020	-40492	-77947	-99780	
March 2020	-30489	-48889	-47875	-53388

Table 5.3 Simulation results Option 3: real time estimates for the differences between the trend and the benchmark trends for Unemployed Labour Force, Employed Labour Force and Total Labour Force at the national level. The last four columns contain differences for respectively December, January, February, and March, based on the time series observed until the month specified in the first column.

This simulation shows that Option 1 and 2 give comparable results. Option 3 performs clearly worse compared to the other two options. The reason is that in Option 3 a different parametrisation of the RGB is used, which introduces an additional shock in the trend estimates of about 6,000 for the Unemployed Labour Force, 9,000 for the Employed Labour Force, and 15,000 for the Total Labour Force.

This simulation was conducted in April 2020. Based on these results it was decided that Option 1 or 2 are the most promising options to consider, once the data over April became available in the first week of May. For Option 1, the break due to the loss of CAPI equals the value for $\kappa_t^{[1]}$ at March 2020, obtained with Model (9). This model is applied to the series of the Unemployed, Employed and Total Labour force at the national level and their breakdown in six domains based on the cross classification of gender and three ages classes. Subsequently the discontinuity estimates are made consistent such that the sum of the Employed and Unemployed Labour Force is exactly equal to the Total Labour Force and the sum of the six domains is equal to the estimate at the national level. This is achieved with a Lagrange function as described in [van den Brakel and Krieg \(2015\)](#).

Results are presented in Table 5.4. The variance of the disturbance terms in the random walk for $\kappa_t^{[j]}$ in (10) tends to zero for almost all variables. This implies that the smooth estimates for $\kappa_t^{[j]}$ are time invariant or evolve very gradually over time. There were two exceptions, namely the Employed and Total Labour Force for the domain Women 45-74. Here the pattern for $\kappa_t^{[j]}$ was very erratic around zero and showed a sudden increase in the last months of the available series. For these two variables the estimate was taken equal to zero. The value after applying Lagrange is shown in Table 5.4.

In general there was a strong correlation between the slope disturbance terms of the trend of the LFS series and the claimant counts. For the Unemployed Labour Force the ML estimate for the correlation was always higher than 0.95, but always lower than 1.0. For the Employed Labour Force the ML estimate for the correlation was always equal to -1.0, with the exception of Men 45-74, where no correlation could be detected. For the Total Labour Force the estimate for the correlation is -1 at the national level, Men 15-24, and Women 15-24. The correlation was estimated at -0.7 for Women 25-44 and zero for the remaining three domains.

	Differences first wave with and without CAPI					
	Unempl. LF		Empl. LF		Total LF	
National	-20848	(2555)	35052	(4206)	14203	(4125)
Men 15-24	-8494	(3023)	-9903	(2052)	-18396	(2128)
Women 15-24	-7097	(3469)	-8140	(1950)	-15236	(2051)
Men 25-44	-11539	(1059)	29000	(1851)	17461	(4097)
Women 25-44	-5268	(884)	36243	(2711)	30976	(8651)
Men 45-74	5739	(1083)	-3325	(6413)	2415	(6543)
Women 45-74	5809	(2182)	-8824	(11774)	-3015	(10273)

Table 5.4 Differences first wave with and without CAPI under Option 1, estimated with Model (9) with the standard errors in brackets. Estimates are numerically consistent using a Lagrange function.

Based on the observations obtained in April 2020, estimates for the discontinuities under Option 2 are made, i.e. discontinuities since CAPI households in the first wave participate via CATI or refuse to participate. These estimates are obtained with Model (13) using time series observed up until and including April 2020. Estimates are summarized in Table 5.5. Similarly to Option 1, these estimates are made numerically

consistent with a Lagrange function.

The estimates for $\beta_t^{[3,1]}$ in Model (13) are, especially at the national level, more or less similar to the results observed for $\kappa_t^{[1]}$ under Option 1 with Model (9). The ML estimates for the correlation between the slope disturbance terms of the trend of the LFS series and the claimant counts under Model (13) are very similar to the results observed under Model (9).

	Discontinuities first wave under Option 2					
	Unempl. LF		Empl. LF		Total LF	
National	-22707	(14082)	40236	(23181)	17529	(23578)
Men 15-24	-4533	(8741)	-609	(11734)	-5142	(10977)
Women 15-24	-6265	(7082)	-20980	(13018)	-27246	(13094)
Men 25-44	-10657	(5088)	27548	(9146)	16890	(8497)
Women 25-44	-9207	(3764)	41853	(9954)	32644	(11185)
Men 45-74	-187	(4053)	7723	(13874)	7536	(12620)
Women 45-74	8144	(3420)	-15297	(14439)	-7153	(13676)

Table 5.5 Discontinuities first wave under Option 2 if CAPI households participate via CATI or refuse, estimated with Model (13) with the standard errors in brackets. Estimates are numerically consistent using a Lagrange function.

Comparing Table 5.4 with Table 5.5, it can be concluded that the point estimates are more or less similar, but the standard errors of the discontinuities under Option 2 are much larger compared to Option 1. The interpretation of this result is as follows. About 8% of the people in the first wave assigned to CAPI agreed to complete a questionnaire via CATI. Normally this response is around 45%. This implies that the discontinuity in Option 2 is mainly due to the selective non-response of the people assigned to the CAPI mode and only to a very limited extend due to the difference in measurement bias between CAPI and CATI response. As a result the point estimates of the discontinuities under Option 2 are approximately similar to the differences between the first wave with and without CAPI under Option 1. Under Option 1, these differences are estimated based on time series with a length of about seven years. The discontinuities under Option 2 are based on one observation of April 2020. Therefore the standard errors under Option 2 are much larger compared to Option 1. Based on this information it was decided in the first week of May, that the official monthly labour force figures for the second quarter of 2020 would be based on Option 1. If during the second quarter of 2020 the response under the people assigned to the CAPI mode substantially increases, it would be reconsidered to use Option 2 for the third quarter of 2020 and also to revise the publications for the second quarter. Therefore the figures during the second quarter were published as provisional figures that might be revised. During May and June the response of the people assigned to CAPI in the first wave remained low (around 8%). Therefore Option 2 has never been reconsidered and the initial publications for the second quarter have not been revised after all.

The first sample without CAPI respondents in the first wave, drawn in April, entered the second wave in July. Model (9) under Option 1 is applied to the series of the second wave with and without CAPI respondents from the first wave, to estimate the impact of losing the CAPI households in the second wave. Results are provided in Table 5.6. The estimates for $\kappa^{[2]}$ obtained for June 2020 in Model (9) were used as an estimate for $\beta^{[3,2]}$ in Model (7). In July and August, it was observed that the filtered trends and

signals under Model (7) that models the impact of losing CAPI households in the second wave are approximately equal to the filtered estimates under (7) that only models the loss of CAPI in the first wave. The reason is that the RGB in the second wave absorbs the loss of CAPI households in the second wave. In order to keep the production model as parsimonious as possible it was therefore decided to include a component to account for the loss in CAPI in the first wave only.

	Differences first wave with and without CAPI					
	Unempl. LF		Empl. LF		Total LF	
National	3551	(4401)	62941	(6742)	66492	(6236)
Men 15-24	1761	(5433)	-4636	(2895)	-2875	(3289)
Women 15-24	-3169	(1384)	1292	(4102)	-1877	(2790)
Men 25-44	-8579	(1684)	43674	(7700)	35095	(8680)
Women 25-44	-5280	(1573)	46217	(3324)	40937	(8922)
Men 45-74	8621	(1419)	-3658	(3630)	4963	(3062)
Women 45-74	10198	(3604)	-19948	(15678)	-9750	(6446)

Table 5.6 Differences second wave with and without CAPI under Option 1, estimated with Model (9) with the standard errors in brackets. Estimates are numerically consistent using a Lagrange function.

6 Modeling increased population dynamics during the COVID-19 pandemic

The lockdown also had a strong impact on the real development of the Employed, Unemployed and Total Labour Force. After the recovery of the Great Financial Crisis, the Unemployed Labour Force showed a steady decreasing trend from 2014 until March 2020. The Employed Labour Force and Total Labour Force showed a steady increasing trend. The start of the lockdown marked a sharp turning point in the trend of these series in April 2020. Once the lockdown regulations were relaxed in June 2020 a partial recovery was visible.

It appeared in April 2020 that the trend component (3) was not flexible enough to adapt to the suddenly increased dynamics of the population parameter in the time series Model (7). This model miss-specification became visible since standardized innovations took values around 4 in absolute terms. The most straightforward approach to increase the flexibility of the trend component is to replace the smooth trend model (3) by a local linear trend model. This implies that a level disturbance term is added to the smooth trend model, i.e.

$$\begin{aligned}
 L_t &= L_{t-1} + R_{t-1} + \zeta_t \\
 R_t &= R_{t-1} + \eta_t \\
 \begin{pmatrix} \zeta_t \\ \eta_t \end{pmatrix} &\simeq N \left(\begin{pmatrix} 0 \\ 0 \end{pmatrix}, \begin{pmatrix} \sigma_\zeta^2 & 0 \\ 0 & \sigma_\eta^2 \end{pmatrix} \right)
 \end{aligned} \tag{14}$$

The local linear trend model only marginally increases the flexibility of the trend component and does not solve the model miss-specification after the lockdown. This option is therefore not further considered.

Three different options to adapt the time series model to accommodate for these increased dynamics were considered. The first option is to model a shock in the time series component for the population parameter with a level intervention. This implies that (2) is extended with a similar level intervention component as used for the discontinuities in 2010 and 2012, i.e.

$$\theta_t = L_t + \beta^{COVID} \delta_t^{COVID} + S_t + \epsilon_t,$$

with δ_t^{COVID} a dummy indicator that change from zero to one in April 2020 to model the shock induced by the lockdown and β^{COVID} a regression component. This approach is appropriate if the impact of the lockdown is concentrated in one month, which is not a realistic assumption. Alternatively δ_t^{COVID} can gradually change from zero to one over a period of several months, but at the start of the lockdown it is hard to anticipate what a reasonable pattern for δ_t^{COVID} could be. This option was therefore not further pursued.

The second option is to temporarily increase the flexibility of the trend. The flexibility of the trend is determined by the variance of the slope disturbance terms, i.e. σ_η^2 in (3).

The ML estimate for σ_η^2 directly after the lockdown in April 2020 is based on the dynamics of the population parameter before the start of the COVID-19 crisis and therefore not capable to sufficiently pick up the sharp turning point marked by the lockdown. One way to accommodate for the increased dynamics is to make the variance of the slope disturbance terms time varying. This is achieved by multiplying this variance with a time varying factor, which value is assumed to be known. This implies the following covariance structure for the slope disturbance terms in (3):

$$\eta_t \simeq N(0, k_t \sigma_\eta^2) \tag{15}$$

where k_t is set in advance. Before the start of the lockdown $k_t = 1$. Two months before the lockdown k_t is temporarily increased such that the standardized innovations in the months after the lockdown have reasonable values, say a maximum of 2.2-2.5 in absolute terms for the month after the start of the lockdown and smaller than 2.0 for the preceding months. To minimize the amount of manually and purposefully adjusting the time series estimates, the focus in the months after the lockdown is to bring the value for k_t back to one as soon as possible. Another way to tune the values of k_t is to monitor the values of the in real time computed ML estimates of σ_η^2 . Model (7) with a time constant variance for the slope disturbance terms will accommodate to the increased dynamics induced by the lockdown, by increasing the value for the ML estimate for σ_η^2 . This means that values for estimates of σ_η^2 obtained with the series that end before the lockdown will be smaller than estimates obtained with series that include observations during the lockdown. One way to tune the values for k_t is to increase them until the values of the ML estimates for σ_η^2 are comparable with the estimates obtained with series ending before the start of the lockdown.

Increasing the variance of the slope disturbance terms through factors k_t has the following interpretation. As the variance of the slope disturbance terms increases, the influence of more distant observations on the level of the trend becomes smaller. The proposed approach implies that the filtered estimates attach less weight to the prediction based on observations from the past and more weight to the direct estimates obtained in the last month. This seems reasonable in periods where the world suddenly

changes and becomes incomparable with the past, as was the case with the COVID-19 pandemic.

The third option is to make the variance of the slope disturbance terms time varying by distinguishing two periods which have their own value for the slope disturbance variances, i.e.

$$\begin{aligned}\eta_t &\simeq N(0, \sigma_{\eta,t}^2), \\ \sigma_{\eta,t}^2 &= \begin{cases} \sigma_{\eta,1}^2 & \text{if } t \notin [T_{LD} - 2, \dots, T_{EL}] \\ \sigma_{\eta,2}^2 & \text{if } t \in [T_{LD} - 2, \dots, T_{EL}] \end{cases},\end{aligned}\quad (16)$$

where T_{EL} denotes the end of the period where an increased or different value for the variance of the slope disturbance terms is required. The slope disturbance variances $\sigma_{\eta,1}^2$ and $\sigma_{\eta,2}^2$ are estimated with ML. This option is therefore not applicable directly after the start of the lockdown, since insufficient observations are available after the start of the lockdown. This method is therefore not considered for the production of official statistics during 2020, but it is interesting to compare outcomes under option 2 with this option as a form of evaluation, once sufficient observations are available to estimate $\sigma_{\eta,2}^2$. Another drawback of this approach is that it is difficult to determine the month $t = T_{EL}$ where the period with an increased variance ends.

Another option, not further investigated, is to apply methods from financial econometrics to accommodate for time varying variance. To model time varying volatility in financial returns, Generalized Autoregressive Conditional Heteroscedasticity (GARCH) models are proposed in the financial econometrics literature. These models are not further considered in this paper, since they are intended for time series observed at a much higher frequency that are subject to continuously changing volatility patterns. Also from a practical point of view it was not feasible to change the state-space model currently implemented for the production of official monthly labour force figures for such an approach within a period of one month. For sake of completeness, we nevertheless refer to [Francq and Zakoian \(2010\)](#) and [Harvey \(2013\)](#) for an overview of GARCH models to account for time varying volatility.

When the data over April 2020 became available, it was decided to use the second option, i.e. temporarily increasing the flexibility of the trend via Model (15) to accommodate for the increased population dynamics in combination with Option 1 from Section 4 to accommodate for the loss of CAPI respondents in the model used for the production of monthly labour force figures. In the next section the effect of both adjustments in the model is evaluated by comparing the results under this model with the unadjusted production Model (1) and Model (1) where the flexibility of the trend is temporarily increased. The chosen option is also compared with a model where the trend has separate variance components for the slope disturbance terms for two different periods, i.e. Model (16).

7 Results

In this section results obtained with the original production model are compared with models that account for the loss of CAPI in the first wave, using Option 1 discussed in Section 4, and models that accommodate for the increased dynamics the population parameters, as discussed in Section 6. The following models are compared:

- Model A: unadjusted production Model (1), i.e. a time constant variance structure (3) for the slope disturbance terms and no correction for the loss of CAPI respondents
- Model B: production Model (1) with a time varying variance structure (15) for the slope disturbance terms but no correction for the loss of CAPI respondents
- Model C: Option 1 to account for the loss of CAPI in the first wave, through Model (7), in combination with a time varying variance structure (15) for the slope disturbance terms
- Model D: Option 1 to account for the loss of CAPI in the first wave, through Model (7), in combination with a time varying variance structure (16) for the slope disturbance terms

To motivate the need of a time varying variance for the slope disturbance terms, the standardized innovations under Model A are plotted in Figure 7.1 in black for the Unemployed, Employed, and Total Labour Force at the national level. The start of the lockdown is marked with large innovations (in absolute terms), indicating that in the second quarter of 2020 the model is seriously miss-specified. The in real time computed ML estimates of the hyperparameters of Model A are given in the upper part of Tables 7.1, 7.2, and 7.3 for the Unemployed, Employed and Total Labour Force at the national level for the twelve months during 2020. Estimating the hyperparameters in real time means that the estimates are based on the series observed up until the particular month in the Tables. It can be seen that the model reacts on the increased dynamics of the population parameter with increased values for the variance estimates of the slope disturbance terms (σ_η^2) and with some delay also the population white noise (σ_ϵ^2).

Based on these findings, the variance of the slope disturbance term is made time varying. The factors k_t used in Model B and C are specified in the lower part of Tables 7.1, 7.2, and 7.3 for the Unemployed, Employed, and Total Labour Force at the national level. These values are minimally increased such that the standardized innovations are reduced until they have values just outside their admissible range of 1.96 in absolute terms. The standardized innovations for Model B are plotted with a dashed red line in Figure 7.1. Note that the structure of the smooth trend model (3) implies that the innovations react with a lag of two months on adjustments of the flexibility factor k_t . Therefore, the value of k_t is increased in February to avoid large standardized innovations in April. To avoid a large shock in the variance of the slope disturbance terms from January to February, the value for k_t was also slightly increased in January. The values for k_t were brought back to one as soon as possible, again by looking at the behaviour of the standardized innovations.

The in real time computed ML estimates of the hyperparameters of Model B are given in the lower part of Tables 7.1, 7.2, and 7.3 for the twelve months during 2020. The estimates for the variance of the slope disturbance terms are now more stable over time. There is still a slight increase that can be avoided by using larger values for k_t for longer periods, but from the perspective of minimally increasing the k_t values to have admissible values for the standardized innovations, this was not necessary and therefore not considered.

The ML estimates for the other hyperparameters are very similar under Model A and Model B. The ML estimates for the hyperparameters obtained with Model C, which also account for the loss of CAPI, are similar to the hyperparameter estimates for Model B in the lower parts of Tables 7.1, 7.2, and 7.3. Also the standardized innovations of both models are comparable with each other. These results are therefore omitted to save space.

	Unemployed Labour Force											
St. Dev.	Jan.	Feb.	March	April	May	June	July	Aug.	Sept.	Okt.	Nov.	Dec.
	Model A (production model with time constant variance for the slope disturbance terms)											
Slope (σ_η)	2001.39	1989.41	1952.95	1884.84	1909.50	2234.10	2586.59	2520.21	2314.84	2229.64	2166.99	2212.98
Seas. (σ_ω)	131.64	123.05	114.73	193.76	213.49	315.48	297.41	296.22	320.41	314.69	399.05	417.42
White N. (σ_ϵ)	6393.87	6314.45	6381.10	6731.79	6735.15	6919.48	6413.08	6490.51	7101.74	7402.67	7477.07	7191.07
RGB (σ_λ)	1655.89	1609.37	1660.87	1744.28	1738.18	1717.45	1679.24	1627.98	1702.91	1740.79	1720.89	1808.22
S.Error W1 (σ_{e_1})	1.14	1.14	1.14	1.14	1.14	1.14	1.13	1.13	1.13	1.13	1.14	1.13
S.Error W2 (σ_{e_2})	1.16	1.16	1.17	1.17	1.18	1.18	1.18	1.17	1.17	1.17	1.17	1.17
S.Error W3 (σ_{e_3})	1.11	1.11	1.11	1.10	1.10	1.09	1.10	1.10	1.09	1.09	1.09	1.09
S.Error W4 (σ_{e_4})	1.11	1.10	1.10	1.10	1.10	1.11	1.11	1.11	1.11	1.11	1.11	1.11
S.Error W5 (σ_{e_5})	1.12	1.12	1.12	1.12	1.12	1.12	1.13	1.13	1.13	1.13	1.13	1.13
Rho (ρ)	0.38	0.38	0.38	0.38	0.38	0.38	0.38	0.38	0.38	0.38	0.38	0.38
	Model B (production model with time varying variance for the slope disturbance terms)											
Slope (σ_η)	2001.39	1989.41	1950.02	1991.40	1961.76	2085.15	2013.43	1974.55	1992.40	2034.68	2204.15	2282.66
k_t	10	50	50	10	1	1	1	1	1	1	1	1
$\sqrt{k_t}\sigma_\eta$	6328.94	14067.28	13788.73	6297.38	1961.76	2085.15	2013.43	1974.55	1992.40	2034.68	2204.15	2282.66
Seas. (σ_ω)	131.64	123.05	119.06	160.31	153.71	130.46	160.15	155.65	140.13	85.25	281.21	290.35
White N. (σ_ϵ)	6393.87	6314.45	6346.10	6189.41	6254.74	6445.23	6406.67	6621.62	7101.74	7391.57	7024.05	6691.52
RGB (σ_λ)	1655.89	1609.37	1660.04	1730.38	1744.28	1754.77	1730.38	1654.24	1711.45	1735.58	1708.03	1795.60
S.Error W1 (σ_{e_1})	1.14	1.14	1.14	1.14	1.14	1.13	1.13	1.14	1.13	1.13	1.13	1.13
S.Error W2 (σ_{e_2})	1.16	1.16	1.17	1.17	1.17	1.17	1.17	1.17	1.17	1.16	1.16	1.17
S.Error W3 (σ_{e_3})	1.11	1.11	1.11	1.10	1.10	1.11	1.10	1.11	1.10	1.10	1.10	1.10
S.Error W4 (σ_{e_4})	1.11	1.10	1.10	1.10	1.10	1.11	1.11	1.11	1.11	1.11	1.11	1.10
S.Error W5 (σ_{e_5})	1.12	1.12	1.12	1.12	1.12	1.12	1.12	1.13	1.13	1.13	1.13	1.13
Rho (ρ)	0.38	0.38	0.38	0.38	0.38	0.38	0.38	0.38	0.38	0.38	0.38	0.38

Table 7.1 ML estimates hyperparameters for the Unemployed Labour Force

	Employed Labour Force											
St. Dev.	Jan.	Feb.	March	April	May	June	July	Aug.	Sept.	Okt.	Nov.	Dec.
	Model A (production model with time constant variance for the slope disturbance terms)											
Slope (σ_η)	2579.06	2566.20	2562.35	2853.16	3278.63	3564.15	3333.18	3172.20	3135.93	3118.73	3192.89	3204.08
Seas. (σ_ω)	0.76	0.18	0.46	0.44	0.43	0.28	0.18	0.51	0.68	0.65	0.46	0.15
White N. (σ_ϵ)	10396.05	10437.71	10532.08	12831.79	12691.41	12396.64	12615.49	12615.49	12973.72	13202.75	13163.21	13117.21
RGB (σ_λ)	1551.82	1550.26	1506.71	1512.74	1561.94	1551.04	1668.50	1642.84	1558.04	1548.71	1545.62	1592.69
S.Error W1 (σ_{e_1})	1.06	1.07	1.08	1.06	1.06	1.06	1.07	1.07	1.08	1.08	1.08	1.07
S.Error W2 (σ_{e_2})	1.20	1.20	1.19	1.20	1.20	1.22	1.23	1.22	1.23	1.23	1.24	1.24
S.Error W3 (σ_{e_3})	1.03	1.03	1.05	1.04	1.04	1.05	1.06	1.06	1.06	1.05	1.06	1.07
S.Error W4 (σ_{e_4})	1.02	1.02	1.01	1.03	1.04	1.04	1.05	1.05	1.05	1.05	1.06	1.06
S.Error W5 (σ_{e_5})	0.93	0.93	0.92	0.95	0.95	0.96	0.98	0.98	0.98	0.98	0.98	0.98
Rho (ρ)	0.66	0.66	0.66	0.66	0.67	0.67	0.68	0.67	0.67	0.67	0.68	0.68
	Model B (production model with time varying variance for the slope disturbance terms)											
Slope (σ_η)	2579.06	2566.20	2604.98	2760.54	2759.16	2767.45	2712.65	2529.26	2653.62	2709.94	2712.65	2699.12
k_t	100	1000	1000	100	100	1	1	1	1	1	1	1
$\sqrt{k_t}\sigma_\eta$	25790.61	81150.31	82376.74	27605.38	27591.58	2767.45	2712.65	2529.26	2653.62	2709.94	2712.65	2699.12
Seas. (σ_ω)	0.76	0.18	0.02	0.19	0.40	0.22	0.18	0.31	0.23	0.12	0.10	0.62
White N. (σ_ϵ)	10396.05	10437.71	10344.19	10411.65	10648.57	10637.93	10563.72	9824.95	10364.90	10282.32	10374.76	10406.45
RGB (σ_λ)	1551.82	1550.26	1508.97	1521.85	1542.53	1539.45	1639.56	1642.02	1560.37	1568.20	1562.72	1612.73
S.Error W1 (σ_{e_1})	1.06	1.07	1.08	1.08	1.07	1.07	1.08	1.08	1.10	1.09	1.09	1.09
S.Error W2 (σ_{e_2})	1.20	1.20	1.19	1.20	1.21	1.21	1.22	1.22	1.22	1.22	1.23	1.23
S.Error W3 (σ_{e_3})	1.03	1.03	1.04	1.05	1.05	1.06	1.07	1.07	1.06	1.06	1.06	1.07
S.Error W4 (σ_{e_4})	1.02	1.02	1.02	1.02	1.03	1.03	1.04	1.04	1.04	1.04	1.05	1.06
S.Error W5 (σ_{e_5})	0.93	0.93	0.92	0.93	0.94	0.94	0.96	0.96	0.96	0.95	0.96	0.96
Rho (ρ)	0.66	0.66	0.66	0.66	0.67	0.67	0.68	0.67	0.67	0.67	0.68	0.68

Table 7.2 ML estimates hyperparameters for the Employed Labour Force

	Total Labour Force											
St. Dev.	Jan.	Feb.	March	April	May	June	July	Aug.	Sept.	Okt.	Nov.	Dec.
	Model A (production model with time constant variance for the slope disturbance terms)											
Slope (σ_η)	1841.06	1868.88	1952.95	2245.30	2662.70	2351.00	2099.80	2013.43	2056.16	2027.57	2018.47	2004.39
Seas. (σ_ω)	0.44	37.27	142.25	304.17	1.96	37.25	37.27	206.35	37.27	263.12	252.93	270.86
White N. (σ_ϵ)	14744.06	14817.97	14633.89	14959.41	15177.90	15828.95	16507.92	16140.64	16384.58	15940.14	15924.21	15726.39
RGB (σ_λ)	3448.16	3357.98	3270.16	3437.83	3486.30	3578.13	3803.19	3816.53	3610.48	3563.85	3531.92	3624.95
S.Error W1 (σ_{e_1})	1.03	1.05	1.05	1.04	1.04	1.04	1.05	1.05	1.06	1.06	1.06	1.05
S.Error W2 (σ_{e_2})	1.26	1.26	1.26	1.27	1.26	1.27	1.27	1.27	1.27	1.27	1.28	1.27
S.Error W3 (σ_{e_3})	1.03	1.03	1.04	1.05	1.05	1.06	1.07	1.07	1.07	1.07	1.07	1.08
S.Error W4 (σ_{e_4})	1.02	1.02	1.01	1.03	1.03	1.03	1.04	1.04	1.03	1.03	1.04	1.04
S.Error W5 (σ_{e_5})	1.03	1.03	1.03	1.05	1.05	1.05	1.06	1.06	1.06	1.05	1.05	1.05
Rho (ρ)	0.64	0.64	0.64	0.65	0.65	0.65	0.66	0.65	0.66	0.65	0.66	0.65
	Model B (production model with time varying variance for the slope disturbance terms)											
Slope (σ_η)	1841.06	1868.88	1976.53	2126.21	2059.25	2225.19	2064.40	2033.67	2065.43	2034.68	2018.47	2043.86
k_t	100	1000	1000	1000	100	1	1	1	1	1	1	1
$\sqrt{k_t}\sigma_\eta$	18410.58	59099.24	62503.22	67236.62	20592.47	2225.19	2064.40	2033.67	2065.43	2034.68	2018.47	2043.86
Seas. (σ_ω)	0.44	37.27	37.27	197.27	230.23	37.25	169.63	35.86	0.68	0.88	37.27	37.26
White N. (σ_ϵ)	14744.06	14817.97	14736.69	14372.84	14408.82	14590.06	14575.48	14604.66	13603.68	14423.23	14663.19	14531.81
RGB (σ_λ)	3448.16	3357.98	3270.16	3429.25	3448.16	3496.77	3724.16	3791.80	3583.50	3546.07	3514.30	3606.87
S.Error W1 (σ_{e_1})	1.03	1.05	1.05	1.05	1.05	1.05	1.05	1.05	1.07	1.07	1.07	1.06
S.Error W2 (σ_{e_2})	1.26	1.26	1.26	1.26	1.27	1.27	1.29	1.27	1.27	1.27	1.28	1.27
S.Error W3 (σ_{e_3})	1.03	1.03	1.04	1.05	1.05	1.05	1.06	1.07	1.06	1.06	1.07	1.07
S.Error W4 (σ_{e_4})	1.02	1.02	1.01	1.03	1.03	1.03	1.04	1.04	1.03	1.03	1.03	1.03
S.Error W5 (σ_{e_5})	1.03	1.03	1.03	1.04	1.04	1.04	1.06	1.05	1.05	1.04	1.04	1.04
Rho (ρ)	0.64	0.64	0.64	0.65	0.65	0.65	0.66	0.65	0.66	0.65	0.66	0.65

Table 7.3 ML estimates hyperparameters for the Total Labour Force

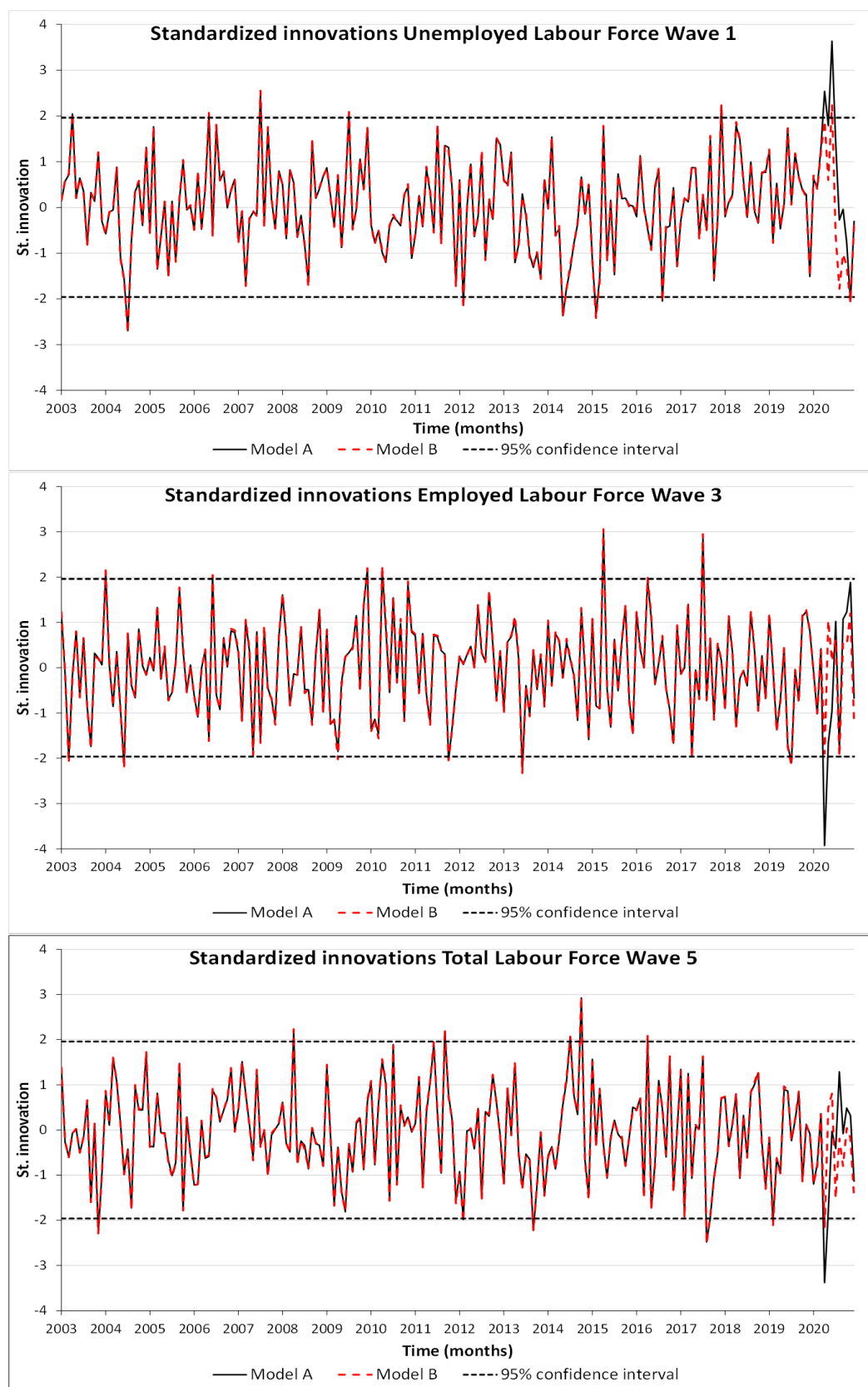


Figure 7.1 Examples of standardized innovations Model A and Model B

In Figure 7.2 filtered trend estimates for the Unemployed, Employed and Total Labour Force under Model A, B, and C are compared together with the GREG input series for the period of January 2018 until December 2020. It is understood that the few CAPI households that respondents via CATI during the lockdown, are not used in the computations of the direct estimates of the input series. The figure for the Unemployed Labour Force also contains the claimant counts. As expected, the filtered trends under the three models are almost equal up until March 2020. Deviations start after the start of the lockdown in April 2020. For all variables the effect of making the trend flexible is clearly larger (Model A versus Model B and C) compared to the effect of compensating for the loss of CAPI (Model B versus Model C). CAPI interviewing stopped in April 2020 and was restarted in September. As a result the filtered trends under Model B and C are almost equal again in the last three months of 2020.

The need to accommodate for the increased dynamics and the loss of CAPI becomes clear if the filtered trend for the Unemployed Labour Force under Model A is compared with the claimant counts. In April there was a lot of uncertainty on the impact of the COVID-19 on the Unemployed Labour Force. On the one hand a sharp increase was to be expected due to the loss of jobs. On the other hand, people may not be available for a job or are temporarily not searching for a job due to the restrictions. From previous economic downturns we expect a strong correlation between the claimant counts and the Unemployed Labour Force. Therefore, the claimant counts were used to assess the unemployment estimates. The increase in the claimant counts was actually also not representing all job losses because many of the people that lost their jobs were not entitled to benefits because they have worked only for a short period. This was especially the case this time because at once a lot of temporary jobs and on-call jobs were terminated. It showed that the claimant counts show a much sharper turn in the slope of the series than the estimates of the Employed and Unemployed Labour Force under model A. This is, in addition to the high values of the standardized innovations, an indication that Model A is miss-specified in the second quarter of 2020 since it cannot pick up the sharp turning point.

The evolution of the figures can be interpreted as follows. At the start of the lockdown the Employed Labour Force dropped with about 150,000 people in April. The Unemployed Labour Force increased with only 35,000 people. A major part of the people that lost their job, left the Labour Force. The Total Labour Force indeed decreased with about 115,000 people. People who lost their job in the second quarter of 2020 were not able to apply or accept a job, due to the strict lockdown regulations in this period. This explains the relatively mild increase of the Unemployed Labour Force and the strong decrease of the Total Labour Force in April. In June the lockdown regulations were relaxed and people were able to apply and accept jobs. This explains the delayed strong increase of the Unemployed Labour Force and the recovery of the Total Labour Force in July. Particularly in the Employed and the Total Labour Force, these period-to-period changes are not visible in the filtered trends under Model A where the flexibility of the trend was not adapted. In the third and fourth quarter of 2020 the Unemployed Labour Force gradually decreases, and the Employed Labour Force gradually increases, which indicates that people start finding paid work again.

The movements from June onwards are not visible in the period-to-period change of the claimant counts. This is because it mainly concerns part-time jobs in branches like retail, hotels, bars, and restaurants. Particularly young people with part-time jobs are not qualified to receive claimant counts after losing this job.

As explained in the previous sections, Model C is used for the production of official monthly figures about the Labour Force. Filtered trends for the Unemployed, Employed and Total Labour Force from January 2003 until December 2020 are shown in Figure 7.3 together with GREG input series of the five waves. The filtered trends are benchmarked to the level of the first wave through the assumption that the RGB of the first wave is zero, at the level of the survey design that is used for data collection from 2012. RGB is particularly visible in the Employed and Total Labour Force. The filtered trends under the designs used before 2012 are corrected for the discontinuities through $\beta^{[1,1]}$ and $\beta^{[1,2]}$ in (7), which explains the deviation of the filtered trend from the input series of the first wave in the first part of the series. Discontinuities are particularly visible in the series of the Unemployed and Employed Labour Force. Since these discontinuities have opposite signs, they cancel out partially in the Total Labour Force. The lockdown in April 2020 marks a sharp turning point in the trends of all three variables.

The standard errors of the filtered trends under Model A and Model C are compared in Figure 7.4. Until the start of the lockdown, the standard errors are almost equal under both models. Modeling the discontinuities due to the redesigns in 2010 and 2012 resulted in a substantial increase of the uncertainty in these periods. After the last redesign in 2012, the standard errors gradually decrease again as more and more information under the new model become available. During the lockdown the standard errors under both models clearly deviate. Making the variance of the slope disturbance terms larger increases the uncertainty of the filtered trend under Model C. Artificially increasing the variance of the slope disturbance terms implies that the time series model relies less on information collected in the past and gives more weight to the GREG estimates observed in the current month. The standard errors reflect this temporarily increased uncertainty, as intended.

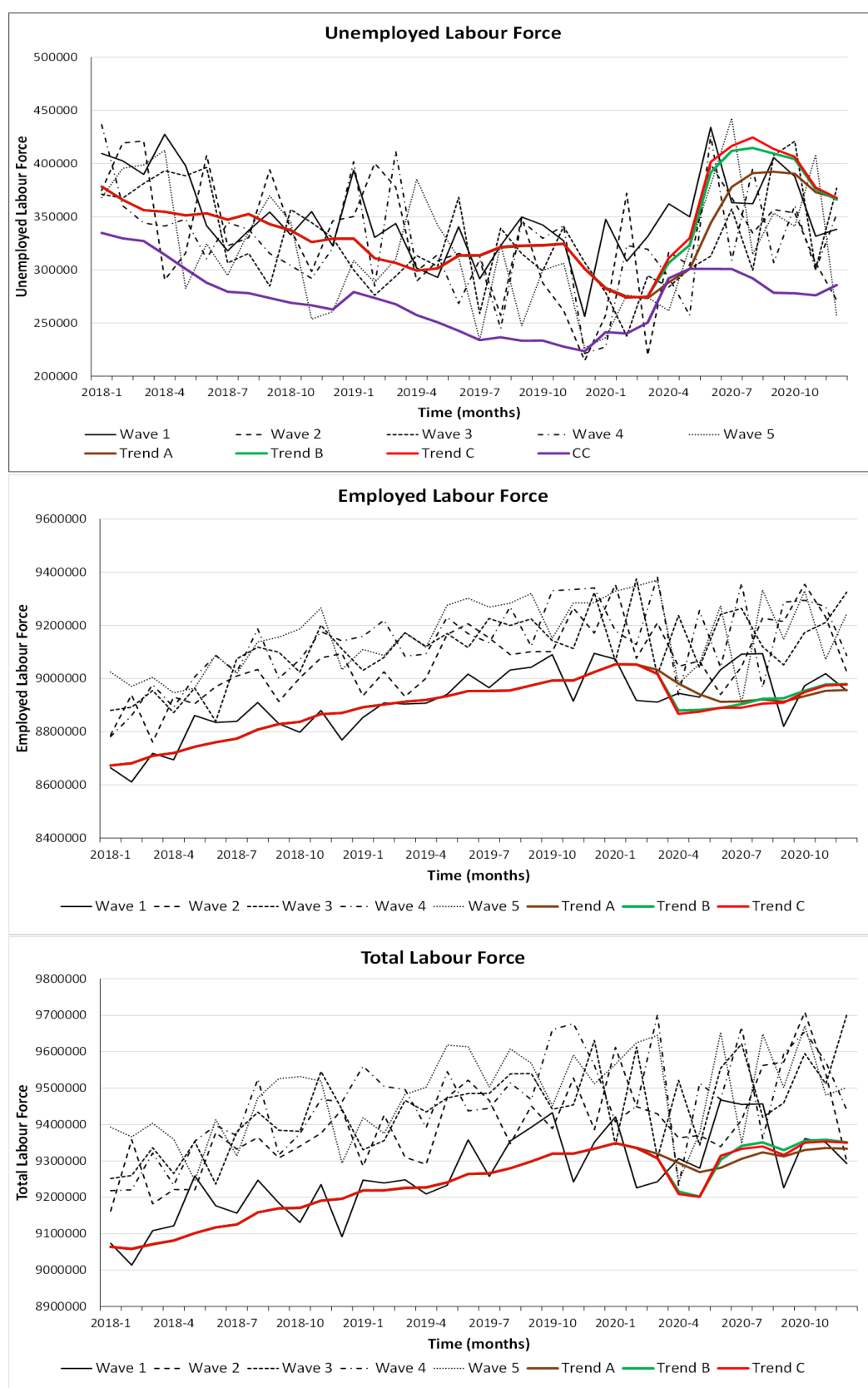


Figure 7.2 Trend estimates under Model A, B, and C for the Unemployed, Employed and Total Labour Force with their input series from January 2018 until December 2020.

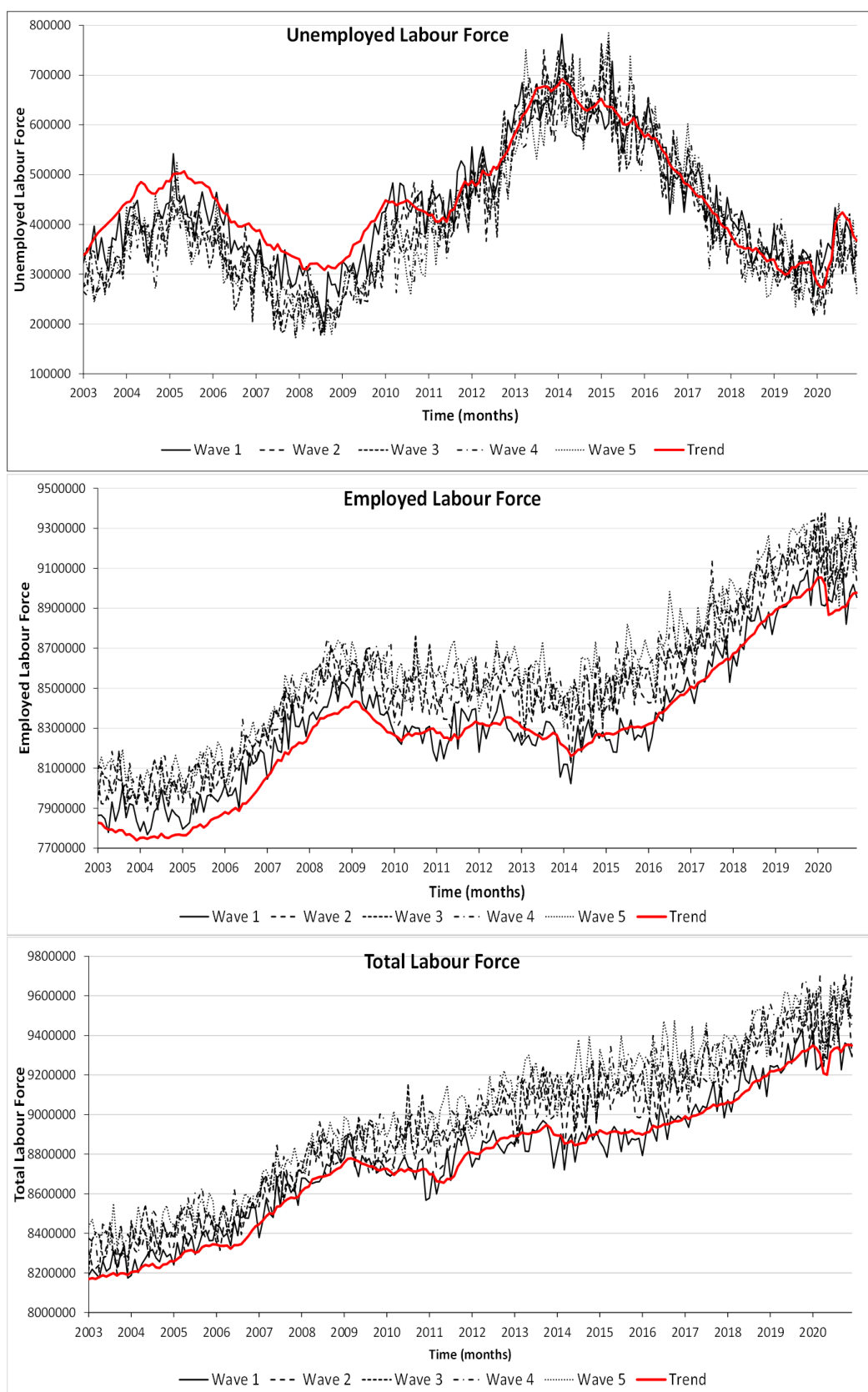


Figure 7.3 Trend estimates under Model C for the Unemployed, Employed and Total Labour Force with their input series from January 2003 until December 2020

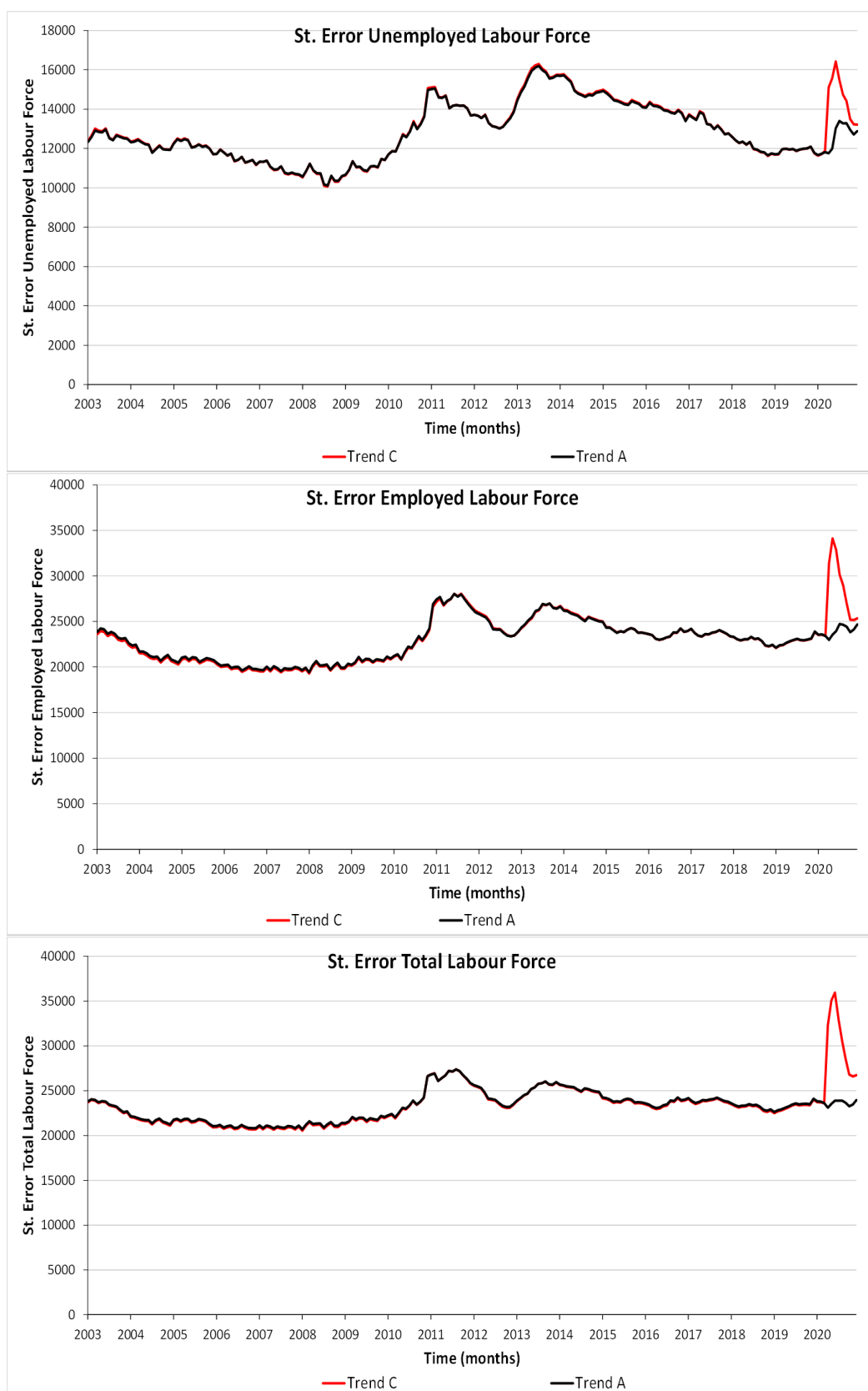


Figure 7.4 Standard error trend estimates

After having observed eight months after the start of the lockdown, it is possible to compare the chosen approach with Model D, which has two separate variance components for the slope disturbance terms, where $\sigma_{\eta,1}^2$ refers to the period before January 2020 and $\sigma_{\eta,2}^2$ refers to the period from January 2020 until December 2020. Table 7.4 contains the ML estimates for both standard deviations of the slope disturbance terms based on the time series observed up until and including December 2020. For the Unemployed Labour Force, the standard deviation of the slope disturbance terms after the lockdown is estimated 10 times larger as for the period before the lockdown. The estimate of 20,152 is also considerably larger than the highest value obtained with the time varying standard deviation, i.e. (15). The estimated standard deviation under the latter approach reached its maximum in February with a value of 14,067, as follows from Table 7.1. For the Employed Labour Force, the standard deviation of the slope disturbance terms after the lockdown is estimated 17 times larger than for the period before the lockdown. For this variable, the estimate of 43,681 remained smaller than the highest value obtained with the time varying standard deviation, i.e. with (15), which attained its maximum value of 82,377 in March (see Table 7.2). For the Total Labour Force, the standard deviation of the slope disturbance terms after the lockdown is estimated more than 20 times larger as for the period before the lockdown. For this variable, the estimate of 42,791 remained smaller than the highest value obtained with the time varying variance for the slope disturbance terms obtained with (15), who attained a maximum value of 67,237 in April (see Table 7.3). For the Employed and Total Labour Force, it appears that the values for k_t of 1000 in Tables 7.2 and 7.3 were chosen too large. An additional analysis indicates that values of 500 instead of 1000 for the months February, March, and April, result in almost equal point and variance estimates for the filtered trends and signals. Results presented in this paper are not adjusted afterwards, since the values specified in Tables 7.1, 7.2 and 7.3, are the values used for the official publications. It appears, on the other hand, that the period for which a separate variance for the slope disturbance terms is required, is shorter than the period assumed in Model D. Defining a shorter period for $\sigma_{\eta,2}^2$, however, results in unreliable ML estimates for $\sigma_{\eta,2}^2$.

Variable	Standard deviation slope disturbance terms	
	Slope before lockdown ($\sigma_{\eta,1}$)	Slope during lockdown ($\sigma_{\eta,2}$)
Unemployed LF	1936.42	20152.74
Employed LF	2548.30	43681.53
Total LF	1871.69	42791.54

Table 7.4 ML estimates standard deviations of the slope disturbance terms of Model D

In Figure 7.5 filtered trend estimates for the Unemployed, Employed and Total Labour Force under Model C and D are compared together with the GREG input series for the period of January 2018 until December 2020. For the Unemployed Labour Force, the trend under Model D is more flexible in quarter 3 and 4 of 2020. For the Employed and the Total Labour Force, the differences between the filtered trend estimates are smaller. The standard errors of the filtered trends under Model D for all three variables are comparable with the peak values obtained under Model C in Figure 7.4 (standard errors for the filtered trend under Model D are not shown). Under Model D the standard errors, however, stay at this high level contrary to Model C, where the standard errors of the filtered estimates rapidly decrease, once the flexibility factor k_t goes back to one.

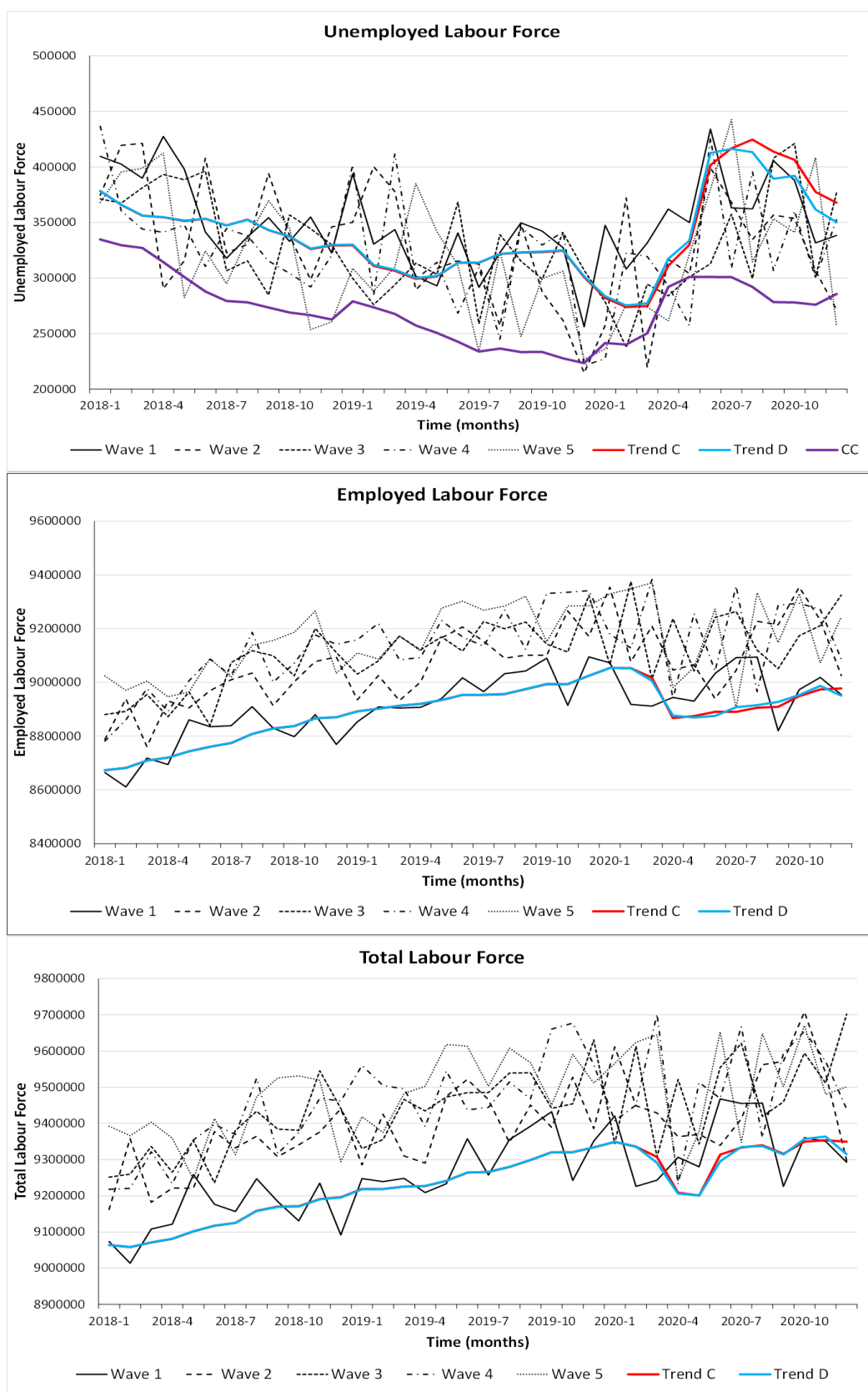


Figure 7.5 Trend estimates under Model C and D for the Unemployed, Employed and Total Labour Force with their input series from January 2018 until December 2020

Model D has several drawbacks which makes this approach inappropriate for this problem. First, it takes a relatively long time before sufficient observations are available to obtain stable ML estimates for the variance of the slope disturbance term for the second period. Second, if the period for which a more flexible trend is required is short, then there will never be enough observations to have reliable ML estimate. On top of that, it is difficult to choose the end of the period for which a more flexible trend is required. In this application it appears that the period where the trend requires increased flexibility is short. The advantage of Model C is that the size of the variance of the slope disturbance terms can be increased temporarily and brought back gradually. Under Model D the variance of the slope disturbance terms appears to be unnecessarily large already in Q4 of 2020. This leads to too volatile trends, while the standard errors of the filtered trends are unnecessarily large.

Finally it is evaluated to which extend two important model assumptions, mentioned in Section 4, are met. The first assumption is that differences between the outcomes in the first wave with and without CAPI is not effected by the lockdown. To evaluate the validity of this assumption, Model (9) is also applied to the time series available until December 2020, where observations for $y_t^{[j]}$ are missing from April until August and are available for the last four months of 2020. The estimates for $\kappa_t^{[j]}$ remain very close to the values reported in Table 5.4, which are based on the time series observed until March 2020. This is a strong indication that the differences did not change after the lockdown. It is also observed that the response rates of the WI and CATI households did not change after the start of the lockdown, which indicates that the assumption that the WI and CATI responses before and after the start of the lockdown are comparable.

8 Discussion

Monthly figures about the Dutch labour force are based on a structural time series model. This estimation approach solves multiple problems. First, it is used as a form of small area estimation to produce sufficiently precise monthly estimates despite small monthly sample sizes. Second, the model accounts for rotation group bias, by benchmarking the model estimates to the level of the first wave. As a result, the estimates based on the rotating panel design, which is introduced in 2000, are comparable with the period before 2000, when the LFS was a cross-sectional survey. Third, the time series model accounts for serial autocorrelation in the sample errors, due to the partial sample overlap of the rotating panel design. Finally, the model accounts for discontinuities that arise due to two major redesigns of the survey process in 2010 and 2012.

The lockdown caused by the COVID-19 pandemic has two effects on the monthly figures of the LFS. It changed the data measurement process because CAPI interviewing stopped, which affects selection and measurement bias in the direct estimates of the monthly labour force figures. At the same time it changed the data generating process, since the dynamics of the population parameters are increased due to the lockdown. The crisis induced by COVID-19 marks a sharp turning point in the evolution of the monthly labour force figures followed by a partial recovery. Since both processes changed at exactly the same time, a method is proposed in this paper to avoid confounding effects due to differences in the measurement process and the data generating process. As a first step, the effect in the outcomes due to the loss of CAPI in

the first wave is estimated with a separate time series model applied to series of direct monthly estimates with and without CAPI responses and a series of claimant counts as an auxiliary series. The difference between the direct estimates with and without CAPI responses are modelled dynamically to allow for gradually changing differences over time. Since the evolution of these differences is constant or almost constant over time, the estimates obtained in the period directly before the start of the lockdown are considered as the best approximation of the impact due to the loss of CAPI in the outcomes of the LFS. In a next step, the time series model used for the production of official monthly labour force figures is extended with a level intervention component that compensates for the loss of CAPI in the input series. The estimate for this effect obtained in the first step, is used as an approximation for the regression coefficient of the level intervention and is treated as if its value is a priori available. The method relies on the strong assumption that the response behaviour of the WI and CATI respondents is not affected by the lockdown. Response analysis of the WI and CATI modes for the months before and after the lockdown support the validity of this assumption. The estimates for the first wave based on the WI, CATI, and CAPI response in the last four months of 2020, also support the assumption that differences between the first wave with and without CAPI did not change after the start of the lockdown. The lockdown also affects the dynamics of the unknown population parameters, which results in a temporal miss-specification of the time series model. The model accommodates for the increased dynamics by making the trend temporarily more flexible. This is achieved by increasing the variance of the slope disturbance terms of the trend.

The empirical results show that the effect of the lockdown on the evolution of the population parameters is much larger than the effect due to the loss of the CAPI responses. Alternative approaches to account for the loss of CAPI responses and the increased dynamics of the population parameters are considered. An evaluation based on the data obtained until December 2020 indicates that there is no indication that an alternative approach should have been chosen. The advantage of the chosen method is that it uses all available information from the past to estimate the effect of the loss of CAPI. Temporarily increasing the flexibility of the trend proved to be a pragmatic solution to accommodate for sudden miss-specification in the time series model. The model temporarily gives more weight to the direct estimates of the current period and less weight to predictions based on passed observations. The increased uncertainty is reflected in a temporal increase of the standard errors of the filtered trend. Finally the chosen approach proved to be manageable to accommodate for unexpected effects in the time series model used for the production of timely monthly labour force figures.

At this point it is unknown what the effect of the COVID-19 pandemic is on the seasonal effects and the autocorrelation of the sampling errors. An advantage of the structural time series model is that seasonal effects are modelled dynamically, which implies that the model can pick up small changes in the seasonal effects. If the model, however, is not capable to pick up a large change in the seasonal effects it might be necessary to adjust the seasonal component. This can be done by modelling seasonal breaks or by making the variance of the seasonal disturbance terms more flexible in a similar way as proposed for the trend. This issue is left as further research since several years of observations after the start of the crisis are required to evaluate possible effects on the seasonal component and the autocorrelation of the sampling error.

Acknowledgement

This paper is reviewed by Marc Smeets. The authors are grateful for his careful reading of a former draft of this paper and providing useful comments.

References

- Bailar, B. (1975). The effects of rotation group bias on estimates from panel surveys. *Journal of the American Statistical Association* 70(349), 23–30.
- Doornik, J. (2009). *An Object-oriented Matrix Programming Language Ox 6*. Timberlake Consultants Press.
- Durbin, J. and S. Koopman (2012). *Time Series Analysis by State Space Methods*. Oxford University Press.
- Francq, C. and J.-M. Zakoian (2010). *GARCH Models*. Wiley and Sons.
- Harvey, A. (2013). *Dynamic Models for Volatility and Heavy Tails*. Cambridge University Press.
- Harvey, A. and J. Durbin (1986). The effects of seat belt legislation on british road casualties: a case study in structural time series modelling. *Journal of the Royal Statistical Society, A series* 149, 187–227.
- Koopman, S. (1997). Exact initial kalman filtering and smoothing for non-stationary time series models. *Journal of the American Statistical Association* 92, 1630–1638.
- Koopman, S., A. Shephard, and J. Doornik (2008). *Ssfpack 3.0: Statistical algorithms for models in state-space form*. Timberlake Consultants, Press London.
- Pfeffermann, D. (1991). Estimation and seasonal adjustment of population means using data from repeated surveys. *Journal of Business & Economic Statistics*, 163–175.
- Pfeffermann, D., M. Feder, and D. Signorelli (1998). Estimation of autocorrelations of survey errors with application to trend estimation in small areas. *Journal of Business & Economic Statistics*, 339–348.
- Särndal, C.-E., B. Swensson, and J. Wretman (1992). *Model Assisted Survey Sampling*. Springer.
- van den Brakel, J. and S. Krieg (2009). Structural time series modelling of the monthly unemployment rate in a rotating panel. *Survey Methodology* 35(2), 177–190.
- van den Brakel, J. and S. Krieg (2015). Dealing with small sample sizes, rotation group bias and discontinuities in a rotating panel design. *Survey Methodology* 41(2), 267–296.
- van den Brakel, J. and R. Roels (2010). Intervention analysis with state-space models to estimate discontinuities due to a survey redesign. *Annals of Applied Statistics* 4, 1105–1138.
- van den Brakel, J., X. M. Zhang, and S.-M. Tam (2020). Measuring discontinuities in time series obtained with repeated sample surveys. *International Statistical Review published online*.

Colophon

Publisher

Statistics Netherlands
Henri Faasdreef 312, 2492 JP The Hague
www.cbs.nl

Prepress

Statistics Netherlands, Grafimedia

Design

Edenspiekermann

Information

Telephone +31 88 570 70 70, fax +31 70 337 59 94
Via contact form: www.cbs.nl/information

© Statistics Netherlands, The Hague/Heerlen/Bonaire 2018.
Reproduction is permitted, provided Statistics Netherlands is quoted as the source